TUM-HEP-339/98
December 1998

Non-Leptonic Two-Body B Decays Beyond Factorization*

Andrzej J. Buras and Luca Silvestrini

Technische Universität München, Physik Department
D-85748 Garching, Germany

Abstract

We present a general scheme and scale independent parameterization of two-body non-leptonic B decay amplitudes which includes perturbative QCD corrections as well as final state interactions in a consistent way. This parameterization is based on the Next-to-Leading effective Hamiltonian for non-leptonic B decays and on Wick contractions in the matrix elements of the local operators. Using this parameterization, and making no dynamical assumption, we present a classification of two-body B decay channels in terms of the parameters entering in the decay amplitudes. This classification can be considered as the starting point for a model-independent analysis of non-leptonic B decays and of CP violating asymmetries. We also propose, on the basis of the large N expansion, a possible hierarchy among the different effective parameters. We discuss the strategy to extract the most important effective parameters from the experimental data. Finally, we establish a connection between our parameterization and the diagrammatic approach which is widely used in the literature.

*Supported by the German Bundesministerium für Bildung und Forschung under contract 06 TM 874 and by the DFG project Li 519/2-2.

1 Introduction

A quantitative description of two-body non-leptonic B decays in the framework of the Standard Model remains as an important challenge for theorists. Simultaneously these decays play a decisive role in the study of CP violation and the determination of the Cabibbo-Kobayashi-Maskawa (CKM) parameters at B-factories and dedicated B-physics experiments at hadron colliders. The studies of these decays should also provide some insight into the long distance non-perturbative structure of QCD.

The basic theoretical framework for non-leptonic B decays is based on the Operator Product Expansion (OPE) and renormalization group methods which allow to write the amplitude for a decay of a given meson B=B_d, B_s, B^+ into a final state F=$\pi\pi$, $K\pi$, DK, KK, ..., generally as follows:

$$\mathcal{A}(B \to F) = \langle F|\mathcal{H}_{\rm eff}|B\rangle = \frac{G_F}{\sqrt{2}} \sum_i V_i^{\rm CKM} C_i(\mu) \langle F|Q_i(\mu)|B\rangle. \tag{1}$$

Here $\mathcal{H}_{\rm eff}$ is the effective weak Hamiltonian, with Q_i denoting the relevant local operators which govern the decays in question. The CKM factors $V_i^{\rm CKM}$ and the Wilson coefficients $C_i(\mu)$ describe the strength with which a given operator enters the Hamiltonian. In a more intuitive language, the operators $Q_i(\mu)$ can be regarded as effective vertices and the coefficients $C_i(\mu)$ as the corresponding effective couplings. The latter can be calculated in renormalization-group improved perturbation theory and are known including Next-to-Leading order (NLO) QCD corrections [1]–[3]. The scale μ separates the contributions to $\mathcal{A}(B \to F)$ into short-distance contributions with energy scales higher than μ contained in $C_i(\mu)$ and long-distance contributions with energy scales lower than μ contained in the hadronic matrix elements $\langle Q_i(\mu)\rangle$. The scale μ is usually chosen to be $O(m_b)$ but is otherwise arbitrary. The μ-dependence of $C_i(\mu)$ has to cancel the μ-dependence of $\langle Q_i(\mu)\rangle$ so that the physical amplitude $\mathcal{A}(B \to F)$ is μ-independent. Similarly, the renormalization scheme dependence of $C_i(\mu)$ cancels the one of $\langle Q_i(\mu)\rangle$. It should be stressed that these cancellations involve generally several terms in the expansion (1).

The great challenge for theorists is a reliable calculation of the matrix elements $\langle Q_i(\mu)\rangle$ in QCD. Unfortunately, due to the non-perturbative nature of the problem, the progress towards this goal has been very slow and it is fair to say that no reliable calculations of the hadronic matrix elements $\langle Q_i(\mu)\rangle$ in QCD exist at present. In the case of two-body non-leptonic B decays, the $\langle Q_i(\mu)\rangle$ cannot in general be calculated from first principles in lattice QCD, due to the Maiani-Testa no-go theorem [4], and even the feasibility of a model-dependent estimate of these matrix elements by numerical simulations still has to be verified [5].

In view of this situation a number of strategies for the calculation of $\mathcal{A}(B \to F)$ have been used in the literature. The most extensive analyses have been done in the factorization approach [6]–[9] in which the hadronic matrix elements $\langle Q_i(\mu)\rangle$ are replaced by the products of the matrix elements of weak currents. The latter can be expressed in terms of various meson decay constants and generally model-dependent form factors. Thus the decay amplitude in this framework is given simply by

$$\mathcal{A}_{\rm I,II} = \frac{G_F}{\sqrt{2}} V^{\rm CKM} a_{1,2}(\mu) \langle Q_{1,2}(\mu)\rangle_F, \tag{2}$$

with

$$a_{1,2}(\mu) = C_{1,2}(\mu) + \frac{1}{N} C_{2,1}(\mu) \tag{3}$$

and N being the number of colours.

Here $\langle Q_i(\mu)\rangle_F$ denote the factorized matrix elements of the current-current operators $Q_{1,2}$ given explicitly in Section 2. The indices I and II distinguish between the so-called class I and class II decays. Since in this approach the matrix elements $\langle Q_i(\mu)\rangle_F$ are scheme- and μ-independent, the resulting amplitudes have these dependencies, which are clearly unphysical.

Two ways of remedying these difficulties have been suggested, which led to the concept of generalized factorization [10]–[14]. In the formulation due to Neubert and Stech [10], the μ-dependent parameters $a_{1,2}(\mu)$ are replaced by the μ- and scheme-independent effective parameters $a_{1,2}^{\rm eff}$. The latter depend formally on $C_i(\mu)$ and non-factorizable contributions to $\langle Q_i(\mu)\rangle$ which are supposed to cancel the μ- and renormalization scheme dependences of $a_i(\mu)$. In this framework there is no explicit calculation of non-factorizable contributions and $a_{1,2}^{\rm eff}$ are treated as free parameters to be extracted from the data. With the assumption of universality and the neglect of a class of non-factorizable contributions represented by penguin diagrams and Final State Interactions (FSI), two-body decays in this approach are parameterized by the two real free parameters $a_{1,2}^{\rm eff}$.

The generalized factorization presented in [11]–[13] is similar in spirit but includes more dynamics than the formulation in [10]. Here the non-factorizable contributions to the matrix elements are calculated in a perturbative framework at the one-loop level. Subsequently these non-factorizable contributions are combined with the coefficients $C_i(\mu)$ to obtain effective μ and renormalization scheme independent coefficients $C_i^{\rm eff}$. The effective parameters $a_i^{\rm eff}$ are given in this formulation as follows:

$$a_1^{\rm eff} = C_1^{\rm eff} + \frac{1}{N^{\rm eff}} C_2^{\rm eff} \qquad a_2^{\rm eff} = C_2^{\rm eff} + \frac{1}{N^{\rm eff}} C_1^{\rm eff} \tag{4}$$

with analogous expressions for $a_i^{\rm eff}$ $(i = 3-10)$ parameterizing penguin contributions. Here $N^{\rm eff}$ is treated as a phenomenological parameter which models the non-factorizable contributions to the hadronic matrix elements. In particular it has been suggested in [11]–[13] that the values for $N^{\rm eff}$ extracted from the data on two-body non-leptonic decays should teach us about the pattern of non-factorizable contributions.

A critical analysis of these two approaches has been presented by us in ref. [15]. In particular we have pointed out that the effective coefficients $C_i^{\rm eff}$ advocated in [11, 13] are gauge and infrared regulator dependent. This implies that the effective number of colours extracted in [11, 13] also carries these dependencies, and therefore it cannot have any physical meaning. Concerning the approach of Neubert and Stech [10], we do not think that this approach is most suitable for the study of non-factorizable contributions to non-leptonic decays. In particular, in the present formulation the contributions from penguin operators, penguin diagram insertions and final state interactions are not included. This implies, for instance, that a large number of penguin-dominated decays cannot be properly described in the present formulation of this approach. Another important issue in the analyses performed in generalized factorization is the dependence on the form factors used. See ref. [16] for a detailed discussion of this point.

Another, more general, approach to non-leptonic decays is the diagrammatic approach, in which the decay amplitudes are decomposed into various contributions corresponding to certain flavour-flow topologies which in the literature appear under the names of "trees", "colour-suppressed trees", "penguins", "annihilations" etc. [17, 18]. Supplemented by isospin symmetry, the approximate $SU(3)$ flavour symmetry and various "plausible" dynamical assumptions the diagrammatic approach has been used extensively for non-leptonic B decays in the nineties.

Recently the usefulness of the diagrammatic approach has been questioned with respect to the

effects of final state interactions. In particular various "plausible" diagrammatic arguments to neglect certain flavour-flow topologies may not hold in the presence of FSI, which mix up different classes of diagrams [19]–[26]. Another criticism which one may add is the lack of an explicit relation of this approach to the basic framework for non-leptonic decays represented by the effective weak Hamiltonian and OPE in eq. (1). In particular, the diagrammatic approach is governed by Feynman drawings with W-, Z- and top-quark exchanges. Yet such Feynman diagrams with full propagators of heavy fields represent really the situation at very short distance scales $O(M_{W,Z}, m_t)$, whereas the true picture of a decaying meson with a mass $O(m_b)$ is more properly described by effective point-like vertices represented by the local operators Q_i. The effect of W, Z and top quark exchanges is then described by the values of the Wilson coefficients of these operators. The only explicit fundamental degrees of freedom in the effective theory are the quarks u, d, s, c, b, the gluons and the photon.

In view of this situation it is desirable to develop another phenomenological approach based directly on the OPE which does not have the limitations of generalized factorization and allows a systematic description of non-factorizable contributions such as penguin contributions and final state interactions. Simultaneously one would like to have an approach that does not lose the intuition of the diagrammatic approach while avoiding the limitations of the latter.

First steps in this direction have been made in refs. [24, 26, 27]. In refs. [24, 27] some of the parameters of the diagrammatic approach have been, in the case of $B \to K\pi$, expressed in terms of matrix elements of local operators. On the other hand in ref. [26] the amplitudes for $B \to \pi\pi$, $B \to K\pi$ and $B \to KK$ have been given in terms of diagrams representing Wick contractions of the operators of the effective Hamiltonian between the relevant hadronic states.

Now the formulation of non-leptonic decays given in ref. [26] involves the explicit expansion of the decay amplitudes in terms of Wick contractions; therefore, with ten operators entering the basic formula (1) and several possible contractions, one ends up with over hundred different contributions, each of them being scale and renormalization scheme dependent.

In the present paper we make the approach of ref. [26] manifestly scale and scheme independent. In this context we introduce a set of effective scale and scheme independent parameters which are given as linear combinations of particular Wick contractions of the operators times the corresponding Wilson coefficients. This reformulation of the approach in [26] in terms of effective parameters results in more transparent formulae for the decay amplitudes than given in [26], establishes some connection with the usual diagrammatic approach and is more suitable for approximations. Moreover we include additional Zweig-suppressed Wick contractions, not considered in the literature, and we study in addition to charmless final states also those including the charm flavour.

The formulae for the effective parameters given here allow in principle their calculation in QCD by means of lattice techniques or other non-perturbative methods. Since this is not possible at present they have to be considered as free parameters to be determined from the data.

It turns out that the full description of two-body B-decays requires the introduction of fourteen flavour-dependent effective parameters. With the help of large N ideas and plausible dynamical assumptions one can argue that several of these parameters play only a minor role in two-body non-leptonic decays.

The approach presented here allows for a general phenomenological description of non-leptonic decays which with more data could teach us about the role of non-factorizable contributions and about the flavour structure of non-leptonic decays. In order to be more predictive some symmetry relations, as $SU(3)$ relations [28], and dynamical input are needed. In this context we would like to

mention an interesting work on non-factorizable contributions to non-leptonic decays within the QCD sum rules approach [29]. We will return to several of these issues in a subsequent publication.

Our paper is organized as follows. In Section 2 we recall the complete effective weak Hamiltonian. In Section 3 we classify various topologies of Wick contractions. We identify fourteen flavour topologies of which only nine have been considered in the literature. The new topologies correspond to Zweig-suppressed transitions. They may play a role only in certain decays but strictly speaking they have to be included for consistency.

In Section 4 we introduce the effective parameters in general terms. In Section 5 we derive by means of a diagrammatic technique the explicit expressions for these parameters including flavour dependence. In Section 6 we propose, using the $1/N$ expansion, a hierarchical structure for the effective parameters. In Section 7 we classify the B_d and B^+ decays into suitable classes and we give explicit expressions for a large number of decays in terms of the most important effective parameters, following the hierarchy proposed in Section 6. In Section 8 we give analogous expressions for B_s decays. The contributions neglected in the analysis of Sections 7 and 8 are collected in Appendix A for completeness. In Section 9 we discuss briefly strategies for the determination of some of the effective parameters from the data and in Section 10 we compare the present approach with the diagrammatic approach of refs. [17, 18]. We end our paper with a brief summary and conclusions. A detailed application of this formalism to two-body B decays, in particular to CP asymmetries, will be presented elsewhere.

2 Effective Hamiltonian

The complete effective weak Hamiltonian for non-leptonic B decays is given by:

$$\begin{aligned}
\mathcal{H}_{\rm eff} \;=\; & \frac{G_F}{\sqrt{2}}\Bigg\{ V_{ub}V_{ud}^*\Big[C_1(\mu)\Big(Q_1^{duu}(\mu)-Q_1^{dcc}(\mu)\Big)+C_2(\mu)\Big(Q_2^{duu}(\mu)-Q_2^{dcc}(\mu)\Big)\Big] \\
& -V_{tb}V_{td}^*\Big[C_1(\mu)Q_1^{dcc}(\mu)+C_2(\mu)Q_2^{dcc}(\mu)+\sum_{i=3,10}C_i(\mu)Q_i^{d}(\mu)\Big] \\
& +V_{ub}V_{us}^*\Big[C_1(\mu)\Big(Q_1^{suu}(\mu)-Q_1^{scc}(\mu)\Big)+C_2(\mu)\Big(Q_2^{suu}(\mu)-Q_2^{scc}(\mu)\Big)\Big] \\
& -V_{tb}V_{ts}^*\Big[C_1(\mu)Q_1^{scc}(\mu)+C_2(\mu)Q_2^{scc}(\mu)+\sum_{i=3,10}C_i(\mu)Q_i^{s}(\mu)\Big] \\
& +V_{ub}V_{cs}^*\Big[C_1(\mu)Q_1^{scu}(\mu)+C_2(\mu)Q_2^{scu}(\mu)\Big]+V_{cb}V_{us}^*\Big[C_1(\mu)Q_1^{suc}(\mu)+C_2(\mu)Q_2^{suc}(\mu)\Big] \\
& +V_{ub}V_{cd}^*\Big[C_1(\mu)Q_1^{dcu}(\mu)+C_2(\mu)Q_2^{dcu}(\mu)\Big]+V_{cb}V_{ud}^*\Big[C_1(\mu)Q_1^{duc}(\mu)+C_2(\mu)Q_2^{duc}(\mu)\Big]\Bigg\}. \qquad (5)
\end{aligned}$$

A basis of operators convenient for our considerations is the one in which all operators are written in the colour singlet form:

$$\begin{aligned}
& Q_1^{d_iu_ju_k}=(\bar b u_k)_{(V-A)}(\bar u_j d_i)_{(V-A)}\,, \quad Q_2^{d_iu_ju_k}=(\bar b d_i)_{(V-A)}(\bar u_j u_k)_{(V-A)}\,, \\
& Q_{J=3,\ldots,10}^{d_i}=\textstyle\sum_q Q_J^{d_iq}\,, \\
& Q_{3,5}^{d_iq}=(\bar b d_i)_{(V-A)}(\bar q q)_{(V\mp A)}\,, \qquad Q_4^{d_iq}=(\bar b q)_{(V-A)}(\bar q d_i)_{(V-A)}\,, \\
& Q_6^{d_iq}=-2(\bar b q)_{(S+P)}(\bar q d_i)_{(S-P)}\,, \qquad Q_{7,9}^{d_iq}=\tfrac{3}{2}(\bar b d_i)_{(V-A)}e_q(\bar q q)_{(V\pm A)}\,, \\
& Q_8^{d_iq}=-3e_q(\bar b q)_{(S+P)}(\bar q d_i)_{(S-P)}\,, \quad Q_{10}^{d_iq}=\tfrac{3}{2}e_q(\bar b q)_{(V-A)}(\bar q d_i)_{(V-A)}\,,
\end{aligned} \qquad (6)$$

where the subscripts $(V \pm A)$ and $(S \pm P)$ indicate the chiral structures, $d_i = \{d, s\}$, $u_i = \{u, c\}$ and e_q denotes the quark electric charge ($e_u = 2/3$, $e_d = -1/3$, etc.). The sum over the quarks q runs over the active flavours at the scale μ. Note that we use here the labeling of the operators as given in [7, 8] which differs from [1]–[3] by the interchange $1 \leftrightarrow 2$.

Q_1 and Q_2 are the so-called current-current operators, Q_{3-6} the QCD-penguin operators and Q_{7-10} the electroweak penguin operators. $C_i(\mu)$ are the Wilson coefficients evaluated at $\mu = O(m_b)$. They depend generally on the renormalization scheme for the operators. For example in the HV scheme one has, including NLO corrections and setting $\overline{m}_{\rm t}(m_{\rm t}) = 170$ GeV, $\mu = 4.4$ GeV and $\alpha_s^{\overline{MS}}(M_Z) = 0.118$ [30]:

$$\begin{array}{ccccc} C_1 = 1.105, & C_2 = -0.228, & C_3 = 0.013, & C_4 = -0.029, & C_5 = 0.009, \\ C_6 = -0.033, & C_7/\alpha = 0.005, & C_8/\alpha = 0.060, & C_9/\alpha = -1.283, & C_{10}/\alpha = 0.266, \end{array} \tag{7}$$

where α is the electromagnetic coupling constant.

The basis in (6) differs from the one used in the NLO calculations in [2, 3] in that some of the operators used there are Fierz conjugates of the ones in (6). This is the case for Q_2, Q_4, Q_6, Q_8 and Q_{10}. As pointed out in [2], the Wilson coefficients evaluated in the NDR scheme (anticommuting γ_5 in $D \neq 4$ dimensions) depend on the form of the operators and the standard Wilson coefficients in the NDR scheme as given in [2, 30] cannot be used in conjunction with the basis (6). On the other hand the HV scheme is Fierz-symmetric and the Wilson coefficients in this scheme calculated in [2, 3] also apply to the basis (6). We will comment at the end of Section 4 on how the expressions for the effective parameters given there have to be modified when the NDR scheme with the basis of [2, 3] is used.

We observe that, unless there is some huge enhancement of their matrix elements, the contributions of the electroweak penguin operators Q_7 and Q_8 are fully negligible. The operators Q_9 and Q_{10} play only a role in decays in which for some dynamical reasons the matrix elements of current-current operators and QCD-penguin operators are strongly suppressed. Generally also the contributions of QCD-penguin operators, especially of Q_3 and Q_5, are substantially smaller than those of the current-current operators Q_1 and Q_2.

3 Classification of Topologies

Following and generalizing the discussion of ref. [26], we classify the various contributions to the matrix elements of the operators Q_i distinguishing the different topologies of Wick contractions as in figs. 1 and 2. We have emission topologies: Disconnected Emission (DE) and Connected Emission (CE); annihilation topologies: Disconnected Annihilation (DA) and Connected Annihilation (CA); emission-annihilation topologies: Disconnected Emission-Annihilation (DEA) and Connected Emission-Annihilation (CEA); penguin topologies: Disconnected Penguin (DP) and Connected Penguin (CP); penguin-emission topologies: Disconnected Penguin-Emission (DPE) and Connected Penguin-Emission (CPE); penguin-annihilation topologies: Disconnected Penguin-Annihilation (DPA) and Connected Penguin-Annihilation (CPA); double-penguin-annihilation topologies: Disconnected Double-Penguin-Annihilation ($\overline{DPA}$) and Connected Double-Penguin-Annihilation ($\overline{CPA}$). The unlabeled line corresponds to a d, u or s quark for B_d, B^+ and B_s decays respectively. The dashed lines represent the operators. The apparently disjoint pieces in the topologies DEA, CEA, DPE, CPE, DPA, CPA, $\overline{DPA}$ and $\overline{CPA}$ are connected to each other by gluons or photons, which are not explicitly

shown. A comment about these topologies is necessary at this point.

These special topologies in which only gluons connect the disjoint pieces are Zweig suppressed and are therefore naively expected to play a minor role in B decays. For this reason, they have been neglected in previous studies [26]. However, as we shall demonstrate in the next Section, they have to be included in order to define scheme and scale independent combinations of Wilson coefficients and matrix elements. We therefore take all of them into account in the following discussion of the effective scheme and scale independent parameters suitable to describe B-decay amplitudes. We will later discuss some approximations that will allow us to reduce the number of parameters necessary to parameterize non-leptonic B decays. On the other hand, if the disjoint pieces are connected by photons, these contributions are automatically at least of $O(\alpha)$.

Our aim is to find a parameterization of the full contribution to the amplitude, including non-factorizable contributions and rescattering effects. Therefore, we will keep all the contributions defined above and consider them to be complex, in order to take into account final state interactions.

The large number of different possible contributions, with different chiralities and flavour structures, requires the introduction of fourteen flavour-dependent, scale and renormalization scheme independent complex parameters in order to be able to describe all decay amplitudes. The fact that the number of effective parameters equals the number of different topologies is accidental. This relatively large number of parameters is necessary if we do not want to make any specific assumption about non-factorizable effects and FSI. Yet, as we will see, this approach offers a transparent classification of various possible contributions and constitutes a good starting point for approximations which would reduce the number of parameters.

In general, the topologies defined above will depend on the flavour and chiral structure, and on the initial and final states. In fact, if factorization were to hold, all this dependence would be taken into account by the factorized matrix element; however, non-factorizable contributions and FSI will in general have a different flavour dependence and cause for example a violation of the universality of the parameters $a_1^{\rm eff}$ and $a_2^{\rm eff}$ introduced in ref. [10] in the framework of generalized factorization. Since here we take into account non-factorizable effects, we keep track of the flavour dependence.

4 Effective Parameters – Generalities

The matrix elements of the operators $Q_i(\mu)$ depend in general on the renormalization scale μ and on the renormalization scheme for the operators. These unphysical dependences are cancelled by those present in the Wilson coefficients $C_i(\mu)$. Due to the mixing under renormalization this cancellation involves generally several operators. From the phenomenological point of view, it is desirable to identify those linear combinations of operator matrix elements times the corresponding Wilson coefficients which are both scheme and scale independent. Such combinations will define the effective parameters to be used in phenomenological applications.

Before entering the details, let us make a few general comments on how the scale and scheme independent effective parameters can be found. It turns out that the flavour structure of the operators Q_1 and Q_2, inserted in the various topologies listed above, and the known behaviour of the operators Q_i under renormalization group transformations, allow us to identify the independent effective parameters.

The first scale and scheme independent combinations of Wilson coefficients and matrix elements

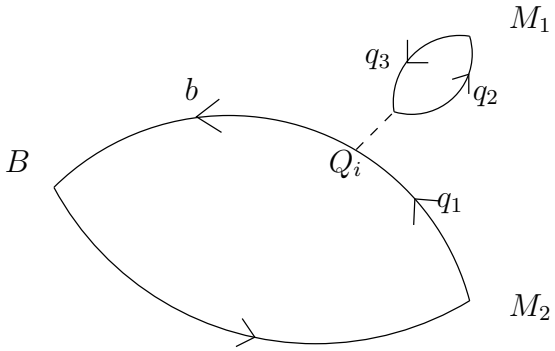

$DE_i(q_3, q_2, q_1; B, M_1, M_2)$

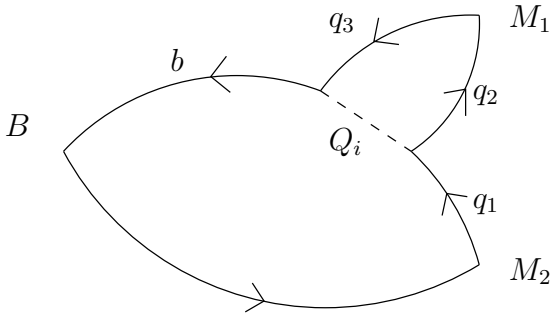

$CE_i(q_3, q_2, q_1; B, M_1, M_2)$

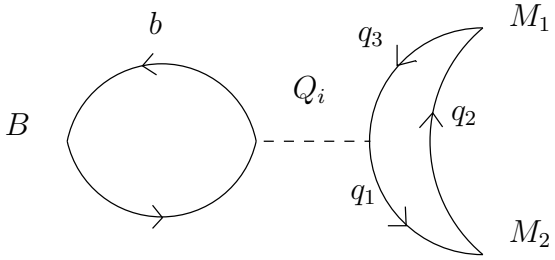

$DA_i(q_3, q_2, q_1; B, M_1, M_2)$

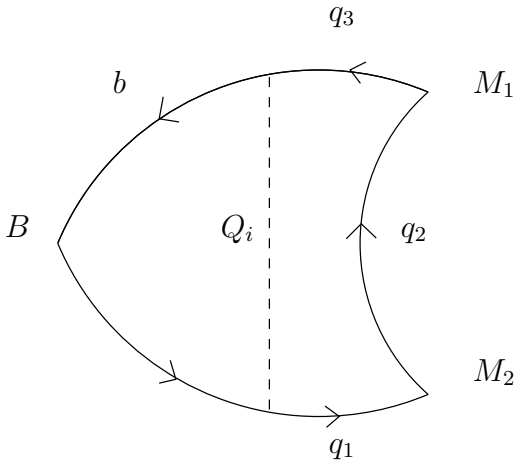

$CA_i(q_3, q_2, q_1; B, M_1, M_2)$

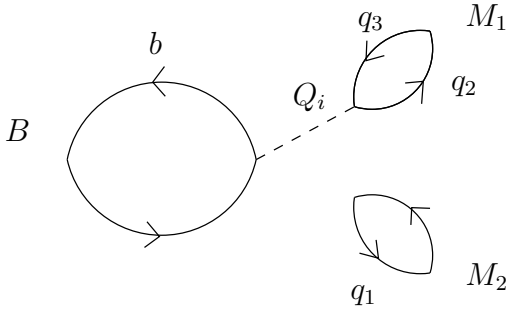

$DEA_i(q_3, q_2, q_1; B, M_1, M_2)$

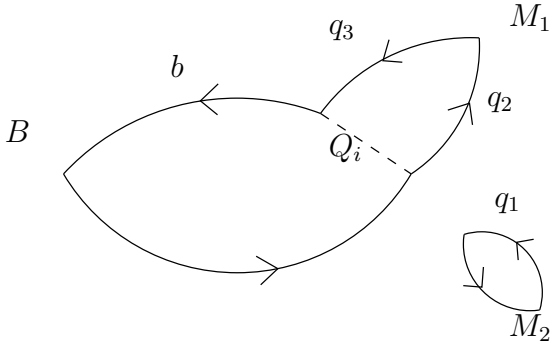

$CEA_i(q_3, q_2, q_1; B, M_1, M_2)$

Figure 1: Emission, annihilation and emission-annihilation topologies of Wick contractions in the matrix elements of operators Q_i.

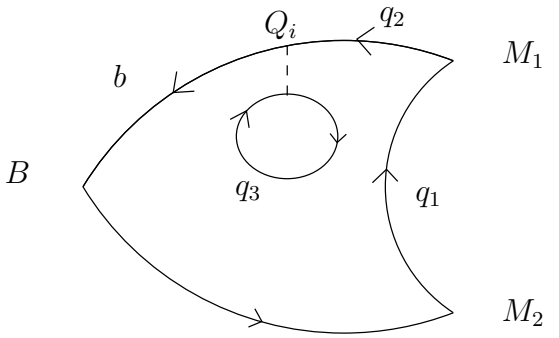

$DP_i(q_3, q_2, q_1; B, M_1, M_2)$

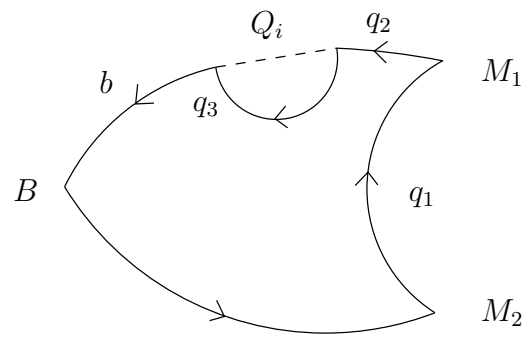

$CP_i(q_3, q_2, q_1; B, M_1, M_2)$

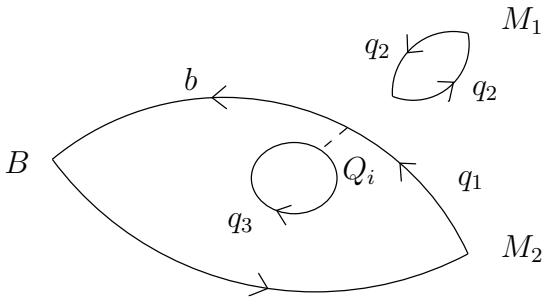

$DPE_i(q_3, q_2, q_1; B, M_1, M_2)$

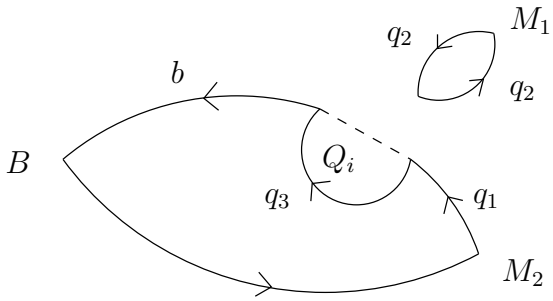

$CPE_i(q_3, q_2, q_1; B, M_1, M_2)$

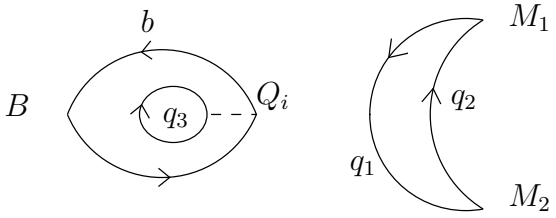

$DPA_i(q_3, q_2, q_1; B, M_1, M_2)$

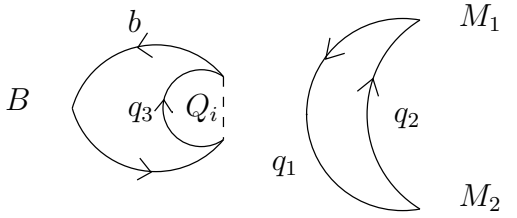

$CPA_i(q_3, q_2, q_1; B, M_1, M_2)$

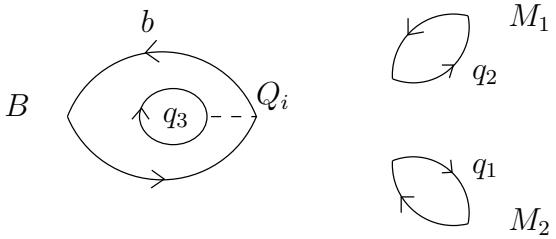

$\overline{DPA}_i(q_3, q_2, q_1; B, M_1, M_2)$

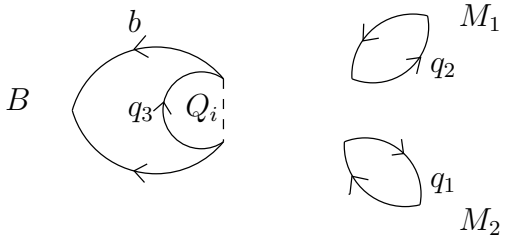

$\overline{CPA}_i(q_3, q_2, q_1; B, M_1, M_2)$

Figure 2: Penguin, penguin-emission, penguin-annihilation and double-penguin-annihilation topologies of Wick contractions in the matrix elements of operators Q_i.

that one can identify correspond to the emission matrix elements of the current-current operators Q_1 and Q_2. Denoting by $\langle Q_i\rangle_{DE}$ and $\langle Q_i\rangle_{CE}$ the insertions of Q_i into DE and CE topologies respectively, one finds two effective parameters

$$\begin{aligned} E_1 &= C_1\,\langle Q_1\rangle_{DE} + C_2\,\langle Q_2\rangle_{CE}\,, \\ E_2 &= C_1\,\langle Q_1\rangle_{CE} + C_2\,\langle Q_2\rangle_{DE}\,. \end{aligned} \tag{8}$$

We have suppressed the flavour variables for the moment. They will be given explicitly in Section 5. E_1 and E_2 are generalizations of $a_1^{\rm eff}\langle Q_1\rangle_F$ and $a_2^{\rm eff}\langle Q_2\rangle_F$ in the formulation of ref. [10].

The reason why two effective parameters are needed can be found by switching off QCD effects, in which case $C_1 = 1$ and $C_2 = 0$. Dependently then on the decay channel considered, the operator Q_1 may contribute either through topology DE or through topology CE, which gives E_1 and E_2 respectively. There are of course channels whose flavour structure allows both $\langle Q_1\rangle_{DE}$ and $\langle Q_1\rangle_{CE}$. These channels can be described by a third effective parameter which is, however, a linear combination of E_1 and E_2. Consequently from the point of view of scale and scheme dependences it cannot be considered as a new effective parameter.

The reason why E_1 and E_2 are scale and scheme independent can be understood in the following manner. Consider operators Q_1 and Q_2 in the case in which all four quark flavours are different. In this case the penguin topologies do not contribute and also the penguin operators cannot be generated by QCD corrections. Choosing in addition channels in which also annihilation contributions are absent, we observe that E_1 and E_2 represent, up to CKM factors, physical amplitudes for the particular channels in question and as such must be scale and scheme independent.

Next, annihilation topologies must be considered. Here we can consider channels in which both emission and penguin topologies as well as penguin operators do not contribute. Analogous arguments as given for E_1 and E_2 allow us to identify two new effective parameters:

$$\begin{aligned} A_1 &= C_1\,\langle Q_1\rangle_{DA} + C_2\,\langle Q_2\rangle_{CA}\,, \\ A_2 &= C_1\,\langle Q_1\rangle_{CA} + C_2\,\langle Q_2\rangle_{DA}\,, \end{aligned} \tag{9}$$

where $\langle Q_i\rangle_{DA}$ and $\langle Q_i\rangle_{CA}$ denote the Q_i-insertions into DA and CA topologies respectively. Due to the flavour structure of operators Q_1 and Q_2, A_1 can only contribute to B^+ decays while A_2 can only contribute to $B_{d,s}$ decays.

It should be stressed that the A_i are independent of the E_i. Indeed, the arguments given above demonstrate that the cancellations of scheme and scale dependences take place separately within emission and annihilation topologies when only current-current operators Q_1 and Q_2 are considered.

The last class of non-penguin contractions that we consider corresponds to the insertion of Q_1 and Q_2 into emission-annihilation topologies, denoted by DEA and CEA in fig. 1. Proceeding as above, we can identify two new effective parameters:

$$\begin{aligned} EA_1 &= C_1\,\langle Q_1\rangle_{DEA} + C_2\,\langle Q_2\rangle_{CEA}, \\ EA_2 &= C_1\,\langle Q_1\rangle_{CEA} + C_2\,\langle Q_2\rangle_{DEA}. \end{aligned} \tag{10}$$

As in the case of A_1 and A_2, due to the flavour structure of Q_1 and Q_2, EA_1 can only contribute to B^+ decays while EA_2 can only contribute to $B_{d,s}$ decays.

We next turn to penguin contractions of current-current operators and matrix elements of penguin operators. Several arguments can be given to conclude that these two types of contributions should be combined in order to obtain scale and scheme independent effective parameters.

First of all let us recall that the Wilson coefficients $C_1(\mu)$ and $C_2(\mu)$ are independent of the presence of penguin operators. The same applies for the insertions of Q_1 and Q_2 into emission and annihilation topologies. Consequently the scale and scheme independent effective parameters E_1, E_2, A_1, A_2, EA_1 and EA_2 are unaffected by the presence of penguin operators. This means that the sum of the remaining contributions to a physical amplitude, that is of penguin contractions of Q_1 and Q_2 and matrix elements of penguin operators, should be separately scheme and scale independent.

In order to see this more clearly let us focus on $b \to s\bar{d}d$ decays. Consider first $\mathcal{H}_{\rm eff}$ to be evaluated at a scale $\mu_1 > m_c$. At this scale, we have penguin insertions of current-current operators containing two charm quarks ($Q^{scc}_{1,2}$) in penguin, penguin-emission, penguin-annihilation and double-penguin-annihilation topologies. In addition, we have emission, annihilation and emission-annihilation matrix elements of penguin operators (Q^{s}_{3-10}). Now take instead $\mathcal{H}_{\rm eff}$ computed at a scale $\mu_2 < m_c$: the operators $Q^{scc}_{1,2}$ have disappeared, and the coefficients of operators Q^{s}_{3-10} have changed in such a way as to compensate for the absence of $Q^{scc}_{1,2}$.

Now similarly to the sets (E_1, E_2), (A_1, A_2) and (EA_1, EA_2) one can find four effective "penguin"-parameters P_1, P_2, P_3 and P_4. The explicit expressions for them will be derived below. Here we just want to relate these parameters to the penguin topologies introduced in Section 3:

1. P_1 involves the insertions of Q_1 and Q_2 into CP and DP topologies respectively and a particular set of matrix elements of QCD-penguin and electroweak penguin operators necessary for the cancellation of scale and scheme dependences;

2. P_2 involves the insertions of Q_1 and Q_2 into CPE and DPE topologies respectively and a suitable set of matrix elements of QCD-penguin and electroweak penguin operators necessary for the cancellation of scale and scheme dependences;

3. P_3 involves the insertions of Q_1 and Q_2 into CPA and DPA topologies respectively and the corresponding set of matrix elements of QCD-penguin and electroweak penguin operators necessary for the cancellation of scale and scheme dependences;

4. P_4 involves the insertions of Q_1 and Q_2 into $\overline{CPA}$ and $\overline{DPA}$ topologies respectively and the remaining matrix elements of QCD-penguin and electroweak penguin operators which have not been included in P_1, P_2 and P_3.

In spite of the fact that in each case both disconnected and connected topologies are present only four effective parameters exist and not eight. This is related to the fact that the insertions of Q_1 into disconnected penguin topologies and the insertions of Q_2 into connected penguin topologies vanish because of the flavour structure of these operators. This should be contrasted with the insertions of these operators into emission and annihilation topologies, where in each case both connected and disconnected topologies can contribute.

The explicit expressions for the P_1, P_2, P_3 and P_4 parameters are as follows:

$$P_1 \;=\; C_1\langle Q_1\rangle^c_{CP} + C_2\langle Q_2\rangle^c_{DP} + \sum_{i=2}^{5}\Big(C_{2i-1}\langle Q_{2i-1}\rangle_{CE} + C_{2i}\langle Q_{2i}\rangle_{DE}\Big)$$

$$+ \quad \sum_{i=3}^{10}\Big(C_i\langle Q_i\rangle_{CP} + C_i\langle Q_i\rangle_{DP}\Big) + \sum_{i=2}^{5}\Big(C_{2i-1}\langle Q_{2i-1}\rangle_{CA} + C_{2i}\langle Q_{2i}\rangle_{DA}\Big)\,, \tag{11}$$

$$\begin{aligned} P_2 &= C_1\langle Q_1\rangle^c_{CPE} + C_2\langle Q_2\rangle^c_{DPE} + \sum_{i=2}^{5}\Big(C_{2i-1}\langle Q_{2i-1}\rangle_{DE} + C_{2i}\langle Q_{2i}\rangle_{CE}\Big) \\ &+ \sum_{i=2}^{5}\Big(C_{2i-1}\langle Q_{2i-1}\rangle_{CEA} + C_{2i}\langle Q_{2i}\rangle_{DEA}\Big) + \sum_{i=3}^{10}\Big(C_i\langle Q_i\rangle_{CPE} + C_i\langle Q_i\rangle_{DPE}\Big)\,, \end{aligned} \tag{12}$$

$$\begin{aligned} P_3 &= C_1\langle Q_1\rangle^c_{CPA} + C_2\langle Q_2\rangle^c_{DPA} + \sum_{i=2}^{5}\Big(C_{2i-1}\langle Q_{2i-1}\rangle_{DA} + C_{2i}\langle Q_{2i}\rangle_{CA}\Big) \\ &+ \sum_{i=3}^{10}\Big(C_i\langle Q_i\rangle_{CPA} + C_i\langle Q_i\rangle_{DPA}\Big)\,, \end{aligned} \tag{13}$$

$$\begin{aligned} P_4 &= C_1\langle Q_1\rangle^c_{\overline{CPA}} + C_2\langle Q_2\rangle^c_{\overline{DPA}} + \sum_{i=2}^{5}\Big(C_{2i-1}\langle Q_{2i-1}\rangle_{DEA} + C_{2i}\langle Q_{2i}\rangle_{CEA}\Big) \\ &+ \sum_{i=3}^{10}\Big(C_i\langle Q_i\rangle_{\overline{CPA}} + C_i\langle Q_i\rangle_{\overline{DPA}}\Big)\,, \end{aligned} \tag{14}$$

where we have denoted by $\langle Q_i\rangle^c_{CP}$ the insertion of operator Q_i in a CP topology with a c-quark running in the loop (this corresponds to the charming penguin of ref. [26]), and analogously for DP, CPE, DPE, CPA, DPA, $\overline{CPA}$ and $\overline{DPA}$ topologies. We notice that, due to the flavour structure of the penguin-annihilation contributions, P_3 and P_4 cannot contribute to B^+ decays. Moreover P_4 contributes only to final states with two flavour neutral mesons $\bar{q}_1 q_1$ and $\bar{q}_2 q_2$. Similarly P_2 contributes only to states with at least one flavour neutral meson $\bar{q}_2 q_2$.

We also stress that, in order to cancel the scheme and scale dependence of the emission contractions of penguin operators in the first line of the expression (12) for P_2, one is forced to introduce the CPE, DPE, CEA and DEA topologies that also contribute to P_2. Analogously, to cancel the scheme and scale dependence of the annihilation contractions of penguin operators in the first line of the expression (13) for P_3, one has to consider the CPA and DPA topologies that also contribute to P_3. Finally, when considering the insertion of penguin operators in the CEA and DEA topologies (first line of the expression (14) for P_4), one has to introduce $\overline{CPA}$ and $\overline{DPA}$ Wick contractions to ensure the scheme and scale dependence of P_4. Therefore, the Zweig-suppressed CPE, DPE, CEA, DEA, CPA, DPA, $\overline{CPA}$ and $\overline{DPA}$ topologies are all needed to obtain a complete scheme and scale independent result.

The P_1, P_2, P_3 and P_4 parameters are always accompanied by the CKM factor $V_{tb}V^*_{td_i}$, where $d_i = d, s$. Penguin-type matrix elements are also present in the part of $\mathcal{H}_{\rm eff}$ proportional to $V_{ub}V^*_{ud_i}$. They correspond to penguin contractions of operators $Q_{1,2}$, or, more precisely, of the differences $\Big(Q_1^{d_i uu} - Q_1^{d_i cc}\Big)$ and $\Big(Q_2^{d_i uu} - Q_2^{d_i cc}\Big)$. When these combinations are inserted into penguin topologies, they give rise to a generalization of the GIM penguins of ref. [26]. These scale and scheme independent contributions are the following:

$$\begin{aligned} P_1^{\rm GIM} &= C_1\Big(\langle Q_1\rangle^c_{CP} - \langle Q_1\rangle^u_{CP}\Big) + C_2\Big(\langle Q_2\rangle^c_{DP} - \langle Q_2\rangle^u_{DP}\Big)\,, \\ P_2^{\rm GIM} &= C_1\Big(\langle Q_1\rangle^c_{CPE} - \langle Q_1\rangle^u_{CPE}\Big) + C_2\Big(\langle Q_2\rangle^c_{DPE} - \langle Q_2\rangle^u_{DPE}\Big)\,, \\ P_3^{\rm GIM} &= C_1\Big(\langle Q_1\rangle^c_{CPA} - \langle Q_1\rangle^u_{CPA}\Big) + C_2\Big(\langle Q_2\rangle^c_{DPA} - \langle Q_2\rangle^u_{DPA}\Big)\,, \\ P_4^{\rm GIM} &= C_1\Big(\langle Q_1\rangle^c_{\overline{CPA}} - \langle Q_1\rangle^u_{\overline{CPA}}\Big) + C_2\Big(\langle Q_2\rangle^c_{\overline{DPA}} - \langle Q_2\rangle^u_{\overline{DPA}}\Big)\,, \end{aligned} \tag{15}$$

and they would vanish in the limit of degenerate u and c. The unitarity of the CKM matrix assures that in a given decay P_i is always accompanied by $P_i^{\rm GIM}$ with the same index "i". However, P_i and $P_i^{\rm GIM}$ are always multiplied by different CKM factors and in order to keep the latter factors explicitly one has to consider separately P_i and $P_i^{\rm GIM}$.

It should be stressed that the eight penguin parameters introduced by us differ considerably from the eight penguin parameters $a_i^{\rm eff}$ (i = 3–10) introduced in refs. [11]–[13]. There a given parameter corresponds to a particular operator Q_i and the scale and renormalization scheme dependence is removed by calculating the corresponding matrix elements perturbatively between external quark states. Such an approach suffers from gauge and infrared dependences as stressed by us in ref. [15].

These problems are absent in our approach as each of the penguin parameters P_i receives contributions from all penguin operators Q_{3-10} which mix under renormalization. Consequently the scale and scheme independence of the P_i parameters is automatically assured after the inclusion of penguin contractions of $Q_{1,2}$, without the necessity for any dubious perturbative calculations of matrix elements. Moreover we include all possible penguin topologies, while penguin contractions in penguin-emission and double-penguin-annihilation topologies were not considered in the factorization approach in refs. [11]–[13]. The same applies to emission-annihilation topologies.

If the operator basis is chosen so that the operators are Fierz conjugates of the ones in (6) then the expressions for the effective parameters given above have to be modified appropriately. Denoting generally by $\langle Q_i\rangle_D$ and $\langle Q_i\rangle_C$ the insertions in the disconnected and connected topologies respectively, the modification in question is straightforward. For each Fierz-transformed operator one simply makes the replacements $\langle Q_i\rangle_D \leftrightarrow \langle Q_i\rangle_C$. In particular, in the case of the NDR scheme the modification amounts to

$$\langle Q_{2i}\rangle_D \leftrightarrow \langle Q_{2i}\rangle_C, \qquad i = 1-5. \tag{16}$$

Since the effective parameters are renormalization scheme independent, this transformation does not change their numerical values. On the other hand, in the NDR scheme the operators Q_{2i} appear in the colour non-singlet form and consequently the large N counting is less transparent than in the basis (6).

5 Effective Parameters – Flavour Dependence

In this Section, we discuss in detail the flavour dependence of the effective parameters defined in the previous Section. We give explicit expressions for the effective parameters in terms of the topologies defined in figures 1 and 2. Furthermore, we provide a diagrammatic derivation of the flavour structure of the effective parameters. In this Section, B stands generically for the B_d, B^+ and B_s mesons.

5.1 The Emission Parameters

As we said above, the first scale- and scheme-independent combinations of Wilson coefficients and matrix elements that we can identify correspond to the emission matrix elements of current-current operators (Q_1 and Q_2):

$$\begin{aligned} E_1(q_i,q_j,q_k;B,M_1,M_2) &= C_1 DE_1(q_i,q_j,q_k;B,M_1,M_2) + C_2 CE_2(q_i,q_j,q_k;B,M_1,M_2)\,, \\ E_2(q_i,q_j,q_k;B,M_1,M_2) &= C_1 CE_1(q_i,q_j,q_k;B,M_1,M_2) + C_2 DE_2(q_i,q_j,q_k;B,M_1,M_2)\,. \end{aligned} \tag{17}$$

In order to exhibit the flavour dependence we use here and in the following the notation of figs. 1 and 2 instead of the short-hand notation $\langle Q_i\rangle_T$ (T = topology) used in Section 4. If factorization held, we would obtain

$$\begin{aligned} DE_{1,2}(q_i,q_j,q_k;B,M_1,M_2) &= \langle M_1|(\bar{q}_j q_i)_{(V-A)}|0\rangle\langle M_2|(\bar{b}q_k)_{(V-A)}|B\rangle\,, \qquad (18)\\ CE_{1,2}(q_i,q_j,q_k;B,M_1,M_2) &= \frac{1}{N}DE_{2,1}(q_i,q_j,q_k;B,M_1,M_2)\,, \qquad (19)\end{aligned}$$

and consequently

$$\begin{aligned} E_1(q_i,q_j,q_k;B,M_1,M_2) &= \left(C_1+\frac{1}{N}C_2\right)\langle M_1|(\bar{q}_j q_i)_{(V-A)}|0\rangle\langle M_2|(\bar{b}q_k)_{(V-A)}|B\rangle\ ;\\ E_2(q_i,q_j,q_k;B,M_1,M_2) &= \left(C_2+\frac{1}{N}C_1\right)\langle M_1|(\bar{q}_j q_i)_{(V-A)}|0\rangle\langle M_2|(\bar{b}q_k)_{(V-A)}|B\rangle\,. \qquad (20)\end{aligned}$$

5.2 The Annihilation Parameters

The next scale- and scheme-independent quantities corresponding to the annihilation matrix elements of current-current operators are given by:

$$\begin{aligned} A_1(q_i,q_j,q_k;B,M_1,M_2) &= C_1 DA_1(q_i,q_j,q_k;B,M_1,M_2)+C_2 CA_2(q_i,q_j,q_k;B,M_1,M_2)\,,\\ A_2(q_i,q_j,q_k;B,M_1,M_2) &= C_1 CA_1(q_i,q_j,q_k;B,M_1,M_2)+C_2 DA_2(q_i,q_j,q_k;B,M_1,M_2)\,. \qquad (21)\end{aligned}$$

If factorization held, we would obtain

$$\begin{aligned} A_1(q_i,q_j,q_k;B,M_1,M_2) &= \left(C_1+\frac{1}{N}C_2\right)\langle M_1M_2|(\bar{q}_i q_k)_{(V-A)}|0\rangle\langle 0|(\bar{b}u)_{(V-A)}|B\rangle\ ;\\ A_2(q_i,q_j,q_k;B,M_1,M_2) &= \left(C_2+\frac{1}{N}C_1\right)\langle M_1M_2|(\bar{q}_i q_k)_{(V-A)}|0\rangle\langle 0|(\bar{b}d_l)_{(V-A)}|B\rangle\,,\end{aligned}$$

where $d_l = d, s$. Due to the flavour structure, A_1 only contributes to B^+ decays and A_2 to $B_{d,s}$ decays.

5.3 The Emission-Annihilation Parameters

The last two independent combinations of non-penguin topologies are given by the emission-annihilation matrix elements of current-current operators:

$$\begin{aligned} EA_1(q_i,q_j,q_k;B,M_1,M_2) &= C_1 DEA_1(q_i,q_j,q_k;B,M_1,M_2)+C_2 CEA_2(q_i,q_j,q_k;B,M_1,M_2)\,,\\ EA_2(q_i,q_j,q_k;B,M_1,M_2) &= C_1 CEA_1(q_i,q_j,q_k;B,M_1,M_2)+C_2 DEA_2(q_i,q_j,q_k;B,M_1,M_2)\,. \qquad (22)\end{aligned}$$

5.4 The Penguin Parameters

Each of the parameters P_1, P_2, P_3 and P_4 discussed in Section 4 is obtained by summing the following contributions, with $d_i = \{d, s\}$:

a) two terms containing a given penguin contraction of $Q_1^{d_i cc}$ and $Q_2^{d_i cc}$;

b) all the possible terms obtained by replacing the c-quark loop with the insertion of the penguin operators $Q_{3-10}^{d_i}$ as explained below;

c) the terms obtained by replacing $Q_{1,2}^{d_i cc}$ by $Q_{3-10}^{d_i}$ in the penguin contractions as explained below.

We will now explain how the contributions b) and c) can be obtained, restricting our attention to QCD-penguin operators $Q_{3-6}^{d_i}$. The generalization to electroweak penguin operators is straightforward and will be done subsequently. A diagrammatic representation of how to obtain contribution b) is given in figs. 3–9. Consider the insertion of a current-current operator in a penguin-like diagram in fig. 3. This insertion is clearly scheme and scale dependent. As we discussed above these dependences can be canceled by adding the corresponding contributions of penguin operators. To this end it is useful to develop a diagrammatic correspondence between the penguin insertions of $Q_{1,2}$ and the insertions of penguin operators. In fig. 3 we show the basic procedure which is applied in figs. 4–9. Wherever a gluon can be exchanged between the loop and a quark line, this corresponds to the diagram obtained by replacing the u- or c-quark loop with the insertion of penguin operators. As an example, in fig. 4 we show the correspondence between penguin-type contractions of $Q_{1,2}^{d_i cc}$ and emission-type contractions of $Q_{3-6}^{d_i}$. The same is shown in fig. 5 for annihilation-type contractions of $Q_{3-6}^{d_i}$. In fig. 6 we show the correspondence between penguin-emission contractions of $Q_{1,2}^{d_i cc}$ and emission-type contractions of $Q_{3-6}^{d_i}$. The same is shown in fig. 7 for emission-annihilation contractions of $Q_{3-6}^{d_i}$. In fig. 8 we show the relation between penguin-annihilation contractions of $Q_{1,2}^{d_i cc}$ and annihilation-type contractions of $Q_{3-6}^{d_i}$. In fig. 9 we show the relation between double-penguin-annihilation contractions of $Q_{1,2}^{d_i cc}$ and annihilation-emission contractions of $Q_{3-6}^{d_i}$. The single gluon exchange in figs. 3–9 is just a symbolic representation for the exchange of an arbitrary number of gluons between quark lines.

Using the correspondence rules represented in figs. 3–9, we can obtain contribution b) to the scale- and scheme-independent combinations of penguin-like topologies. As an example, in fig. 10 we show diagrammatically the construction of the b) part of the P_1 contribution defined in Section 4. One starts by considering penguin-like contractions of current-current operators, as depicted in the first box in the figure, which contains the combination $C_1 CP_1(c, d_i, q_2; B, M_1, M_2) + C_2 DP_2(c, d_i, q_2; B, M_1, M_2)$. Then one considers the gluon exchanges drawn in the second box, and substitutes the shaded regions with the corresponding insertions of penguin operators. The resulting third box contains the combination

$$
\begin{aligned}
& \Big(C_3 CE_3(d_i, q_2, q_2; B, M_1, M_2) + C_5 CE_5(d_i, q_2, q_2; B, M_1, M_2) \\
& + C_4 DE_4(d_i, q_2, q_2; B, M_1, M_2) + C_6 DE_6(d_i, q_2, q_2; B, M_1, M_2) \Big) \\
+ \quad & \Big(C_3 CA_3(d_i, q_2, q_1; B, M_1, M_2) + C_5 CA_5(d_i, q_2, q_1; B, M_1, M_2) \\
& + C_4 DA_4(d_i, q_2, q_1; B, M_1, M_2) + C_6 DA_6(d_i, q_2, q_1; B, M_1, M_2) \Big) ,
\end{aligned}
\tag{23}
$$

see eq. (28), where $q_1 = d$, u or s for B_d, B^+ and B_s decays respectively. Analogously, one can build up part b) of P_2 as shown in fig. 11. The starting point is the insertion of Q_1 and Q_2 in penguin-emission diagrams, as shown in the first box in the figure. This corresponds to the combination $C_1 CPE_1(c, d_i, q_2; B, M_1, M_2) + C_2 DPE_2(c, d_i, q_2; B, M_1, M_2)$. Then, a gluon can connect the c-quark loop either with the q_1 line or with the q_2 one, as shown in the second box of fig. 11. In the third box, one replaces the gluon exchange with penguin operators, following figs. 6 and 7, and one obtains the contribution

$$
\begin{aligned}
& \Big(C_3 DE_3(q_2, q_2, d_i; B, M_1, M_2) + C_5 DE_5(q_2, q_2, d_i; B, M_1, M_2) \\
& + C_4 CE_4(q_2, q_2, d_i; B, M_1, M_2) + C_6 CE_6(q_2, q_2, d_i; B, M_1, M_2) \Big)
\end{aligned}
$$

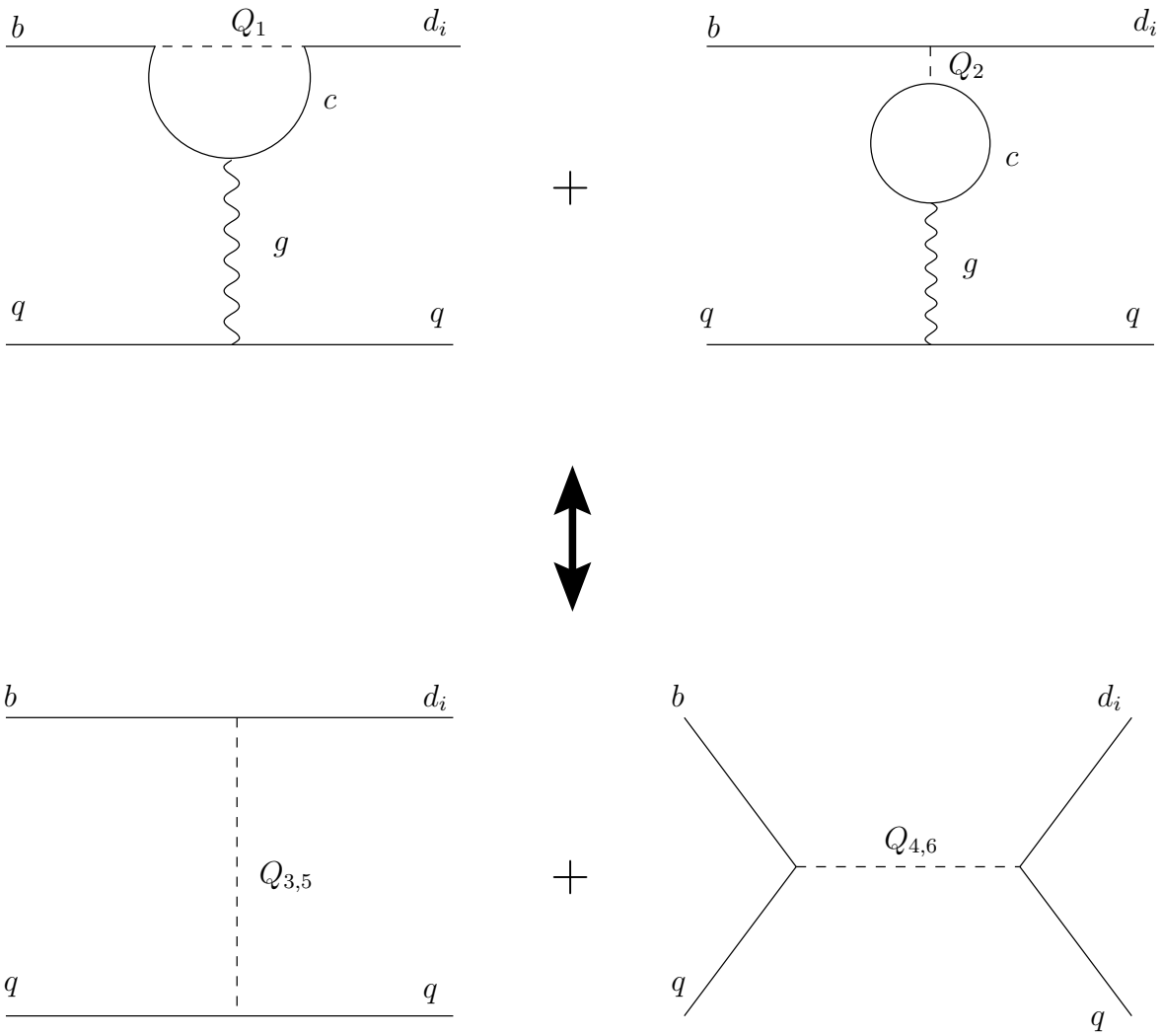

Figure 3: The basic step to relate penguin insertions of current-current operators to emission, annihilation and emission-annihilation insertions of penguin operators. Wherever a gluon can be exchanged between the c-quark loop in the penguin insertions and a quark line, this corresponds to the insertion of a penguin operator.

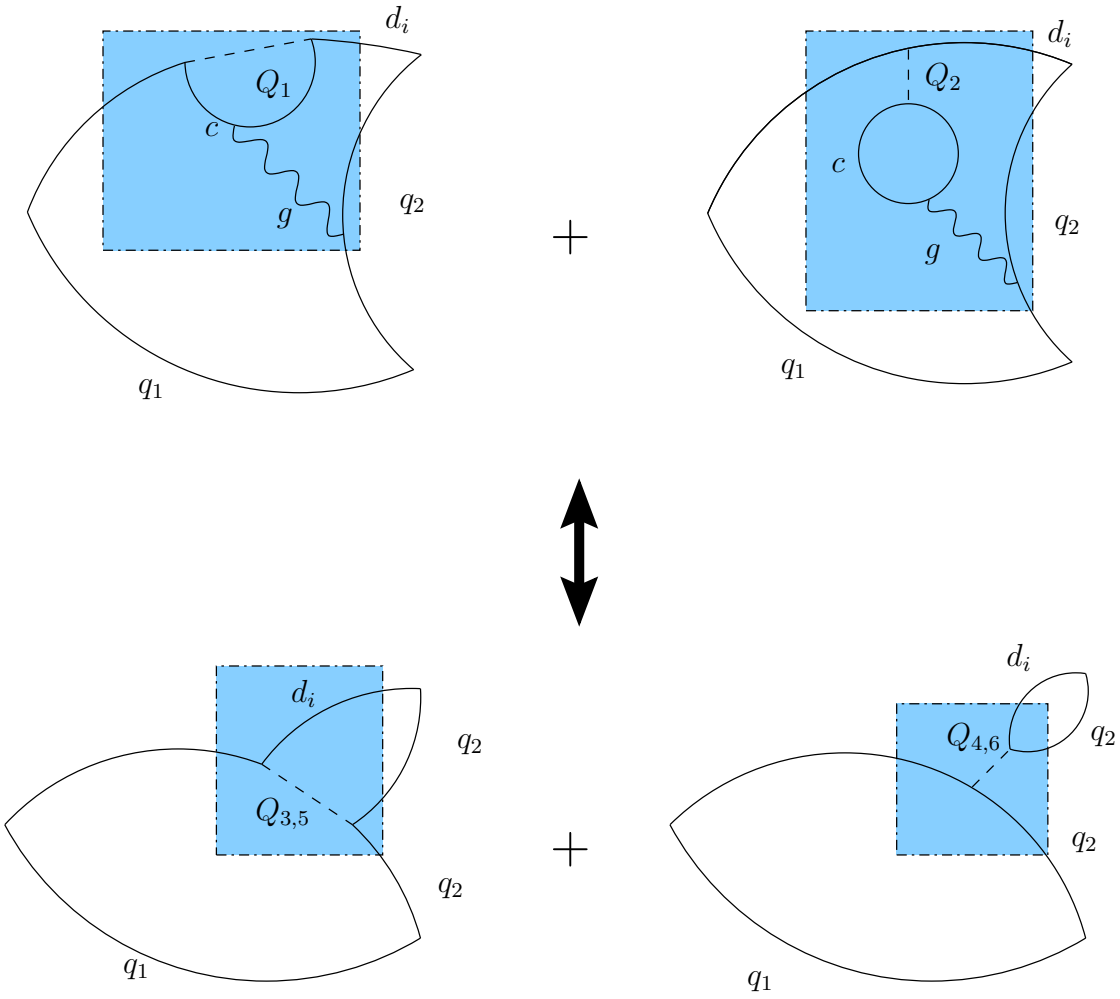

Figure 4: An example of how penguin contractions of current-current operators are related to insertions of penguin operators in emission topologies. First, one notices that a gluon might be exchanged between the c-quark loop and the q_2 line in the penguin topologies (shaded region). Next, using the prescription in fig. 3, one replaces the gluon exchange in the shaded region by the corresponding insertion of a penguin operator.

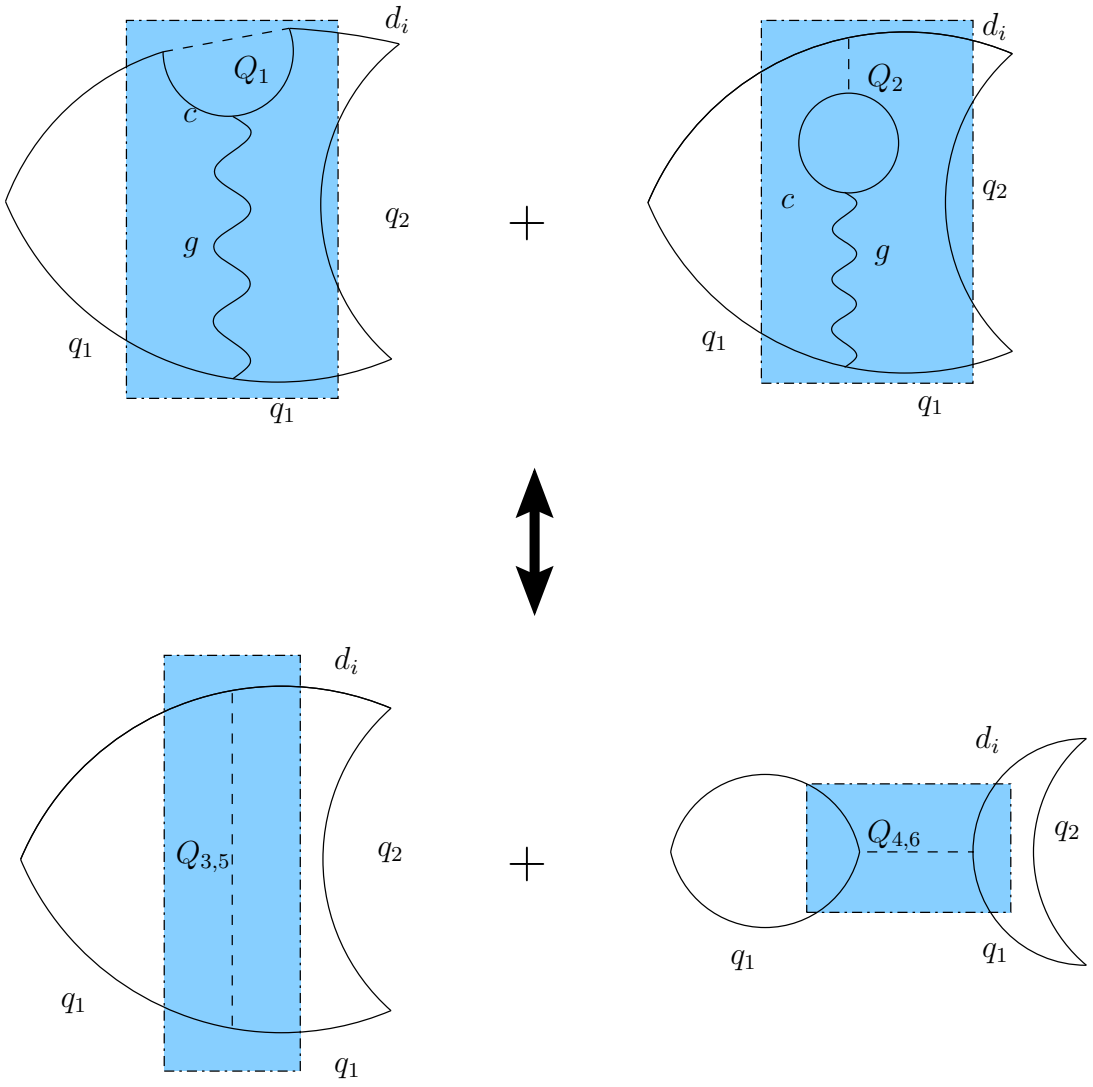

Figure 5: The same as fig. 4, for another possible gluon exchange: in this case, the gluon connects the c-quark loop with the q_1 line in the penguin topology.

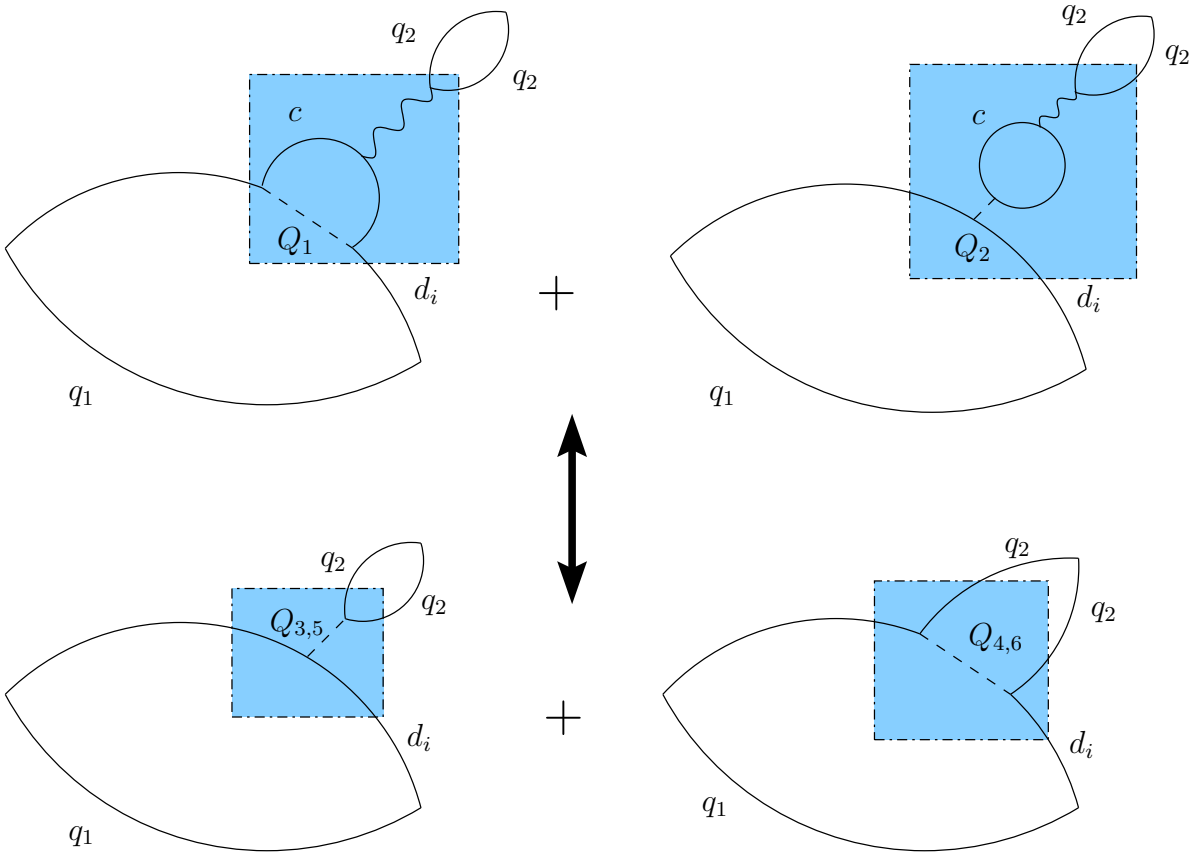

Figure 6: The same as figs. 4–5, for penguin-emission topologies. The shaded region corresponds to a gluon exchange in the penguin topologies, and to the insertion of a penguin operator in the emission topologies.

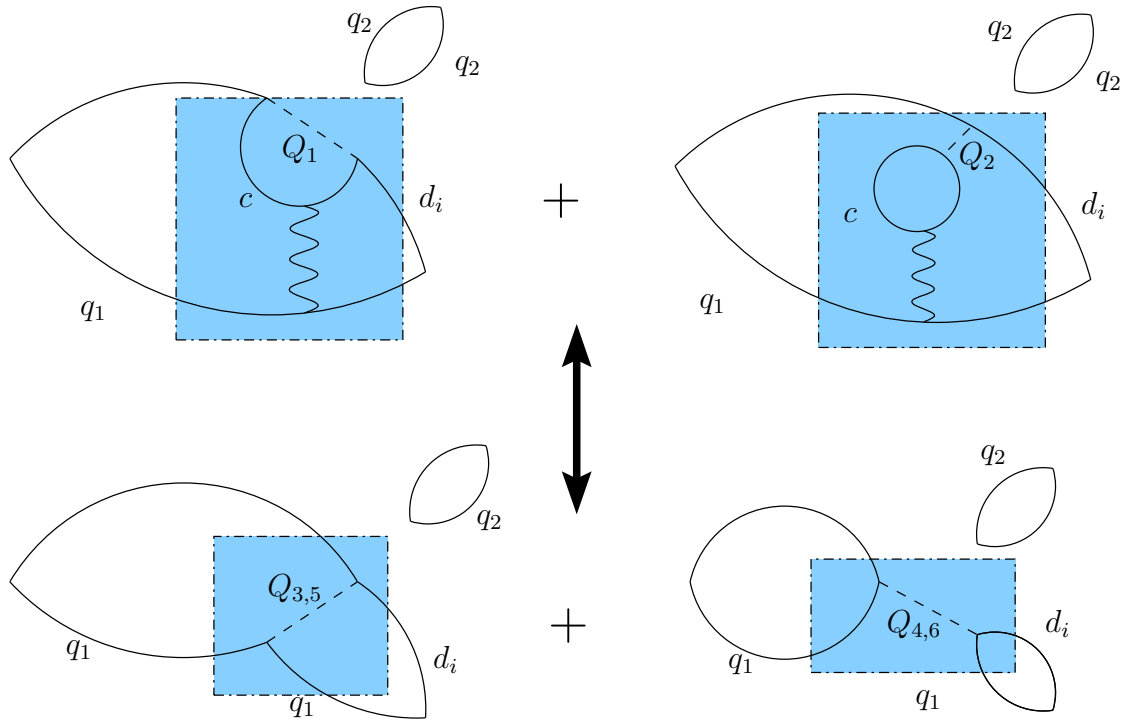

Figure 7: The same as fig. 6, for another possible gluon exchange: in this case, the gluon connects the c-quark loop with the q_1 line in the penguin-emission topology.

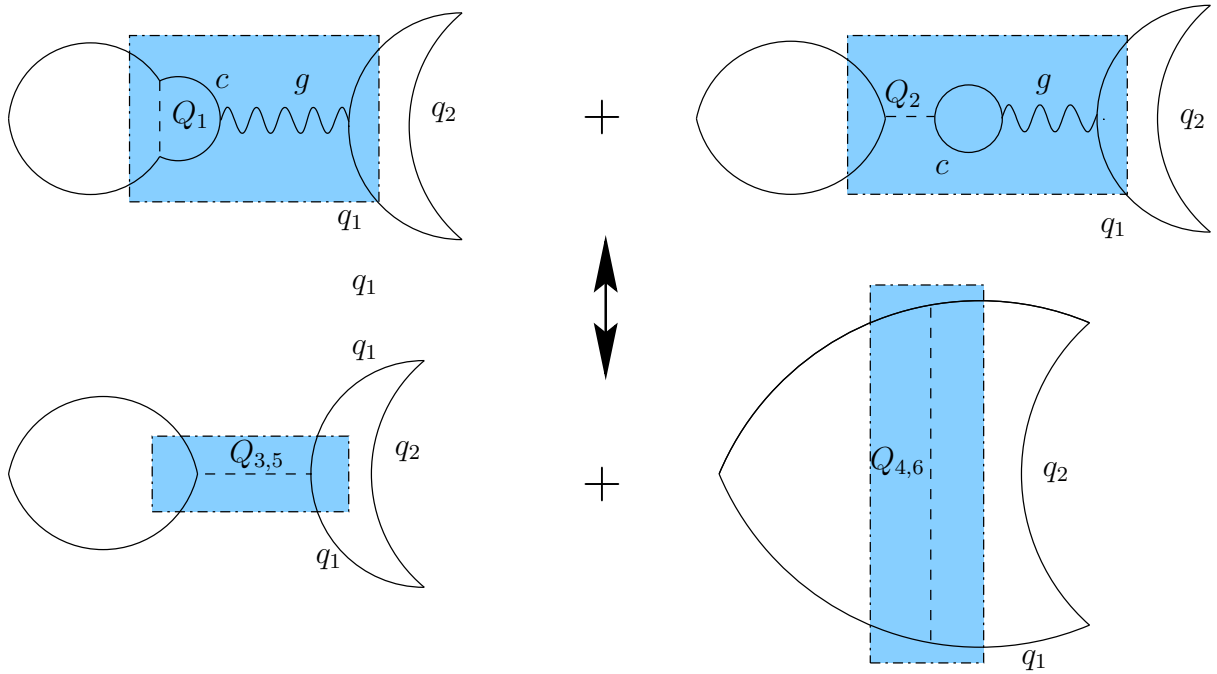

Figure 8: The same as fig. 6, but for penguin-annihilation topologies.

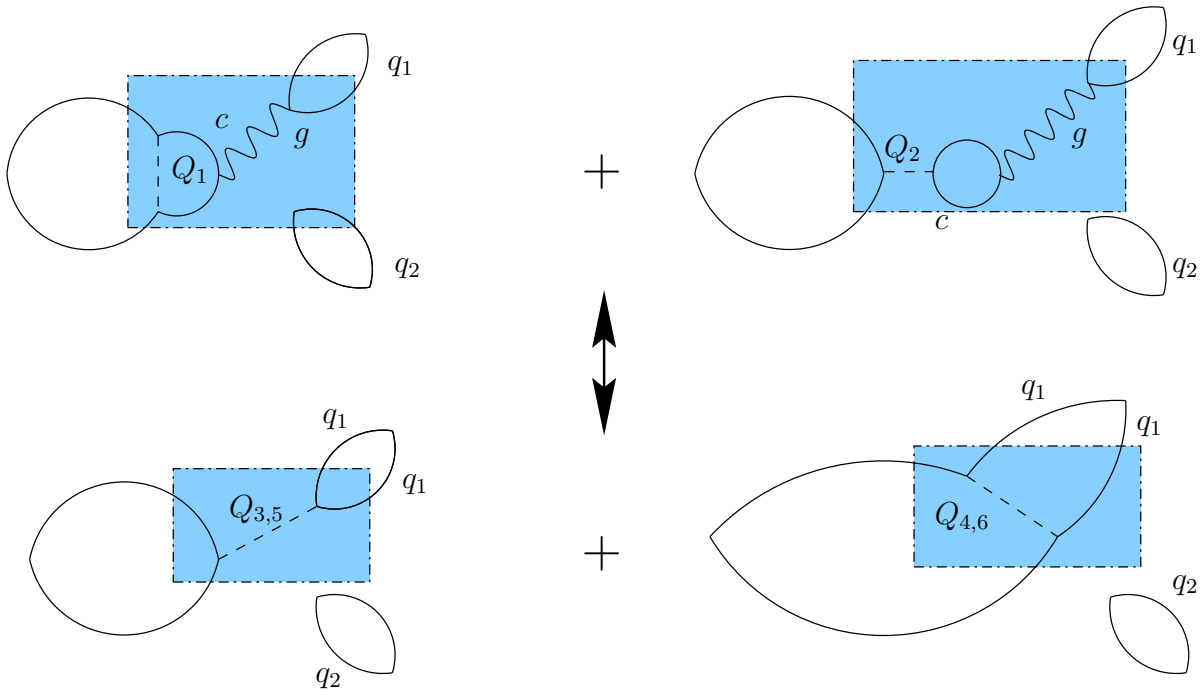

Figure 9: The same as fig. 8, but for double-penguin-annihilation topologies.

$$
\begin{aligned}
+ \quad & \Big(C_3\,CEA_3(d_i,q_1,q_2;B,M_2,M_1) + C_5\,CEA_5(d_i,q_1,q_2;B,M_2,M_1) \\
& + C_4\,DEA_4(d_i,q_1,q_2;B,M_2,M_1) + C_6\,DEA_6(d_i,q_1,q_2;B,M_2,M_1)\Big)\,, \qquad (24)
\end{aligned}
$$

see eq. (29), where $q_1 = d$, u or s for B_d, B^+ and B_s decays respectively. The same is shown in fig. 12 for the P_3 contribution defined in Section 4. Here one starts by the insertion of current-current operators in penguin-annihilation diagrams (first box in the figure), which is given by $C_1\,CPA_1(c,q_2,q_1;B,M_1,M_2)+$ $C_2\,DPA_2(c,q_2,q_1;B,M_1,M_2)$. As in the previous cases, there are two possible types of gluon exchanges, depending on whether the gluon connects the blob to the q_1 or to the q_2 line (second box in fig. 12). Substituting the gluon exchange with insertions of penguin operators, following fig. 8, we get the contribution in the third box, which corresponds to

$$
\begin{aligned}
& \Big(C_3\,DA_3(q_1,q_2,q_1;B,M_1,M_2) + C_5\,DA_5(q_1,q_2,q_1;B,M_1,M_2) \\
& + C_4\,CA_4(q_1,q_2,q_1;B,M_1,M_2) + C_6\,CA_6(q_1,q_2,q_1;B,M_1,M_2)\Big) \\
+ \quad & \Big(C_3\,DA_3(q_2,q_1,q_2;B,M_2,M_1) + C_5\,DA_5(q_2,q_1,q_2;B,M_2,M_1) \\
& + C_4\,CA_4(q_2,q_1,q_2;B,M_2,M_1) + C_6\,CA_6(q_2,q_1,q_2;B,M_2,M_1)\Big)\,, \qquad (25)
\end{aligned}
$$

see eq. (30). Finally, the b) part of P_4 is represented in fig. 13. The starting point here is the insertion of Q_1 and Q_2 in double-penguin-annihilation diagrams, as shown in the first box in the figure. This corresponds to the combination $C_1\overline{CPA}_1(c,q_1,q_2;B,M_1,M_2) + C_2\overline{DPA}_2(c,q_1,q_2;B,M_1,M_2)$. Then, a gluon can connect the c-quark loop either with the q_1 line or with the q_2 one, as shown in the second box of fig. 13. In the third box, one replaces the gluon exchange with penguin operators, following

fig. 9, and one obtains the contribution

$$\begin{aligned}
&\Big(C_3 DEA_3(q_2,q_2,q_1;B,M_1,M_2)+C_5 DEA_5(q_2,q_2,q_1;B,M_1,M_2)\\
&+C_4 CEA_4(q_2,q_2,q_1;B,M_1,M_2)+C_6 CEA_6(q_2,q_2,q_1;B,M_1,M_2)\Big)\\
+\;&\Big(C_3 DEA_3(q_1,q_1,q_2;B,M_2,M_1)+C_5 DEA_5(q_1,q_1,q_2;B,M_2,M_1)\\
&+C_4 CEA_4(q_1,q_1,q_2;B,M_2,M_1)+C_6 CEA_6(q_1,q_1,q_2;B,M_2,M_1)\Big)\,, \qquad (26)
\end{aligned}$$

see eq. (31).

Concerning the c) contribution, it can be obtained by replacing the insertion of current-current operators in penguin topologies with the insertion of penguin operators in the same penguin topologies. An example is shown in fig. 14 for the insertion of $Q_{1,2}^{d_i cc}$ in penguin topologies, where d_i can be either a d or an s quark. The c) contribution is obtained by replacing $Q_{1,2}^{d_i cc}$ with $Q_{3-6}^{d_i}$, as shown in the figure. We remark that the $Q_{3-6}^{d_i}$ operators contain a term with the flavour structure $(\bar{b}d_i)(\bar{d}_i d_i)$. This term contributes with two different Wick contractions, depending on which d_i field is contracted with the $\bar{d}_i$. This extra Wick contraction gives rise to the two diagrams in the last line of fig. 14.

The contributions of electroweak penguins to b) and c) can be obtained by replacing $Q_{3-6}^{d_i}$ with $Q_{7-10}^{d_i}$ using the following correspondence rules:

$$\begin{aligned}
&Q_3 \leftrightarrow Q_9\,, \qquad && Q_4 \leftrightarrow Q_{10}\,,\\
&Q_5 \leftrightarrow Q_7\,, \qquad && Q_6 \leftrightarrow Q_8\,. \qquad (27)
\end{aligned}$$

Applying the above considerations, we are able to identify the scale- and scheme-independent contributions involving penguin operators and penguin contractions:

$$\begin{aligned}
P_1(d_i,q_j;B,M_1,M_2) &= C_1 CP_1(c,d_i,q_j;B,M_1,M_2)+C_2 DP_2(c,d_i,q_j;B,M_1,M_2) \qquad (28)\\
&+\sum_{l=2}^{5}\Big(C_{2l-1}CE_{2l-1}(d_i,q_j,q_j;B,M_1,M_2)+C_{2l}DE_{2l}(d_i,q_j,q_j;B,M_1,M_2)\Big)\\
&+\sum_{l=2}^{5}\Bigg[\sum_q\Big(C_{2l-1}DP_{2l-1}(q,d_i,q_j;B,M_1,M_2)+C_{2l}CP_{2l}(q,d_i,q_j;B,M_1,M_2)\Big)\\
&\qquad +C_{2l-1}CP_{2l-1}(d_i,d_i,q_j;B,M_1,M_2)+C_{2l}DP_{2l}(d_i,d_i,q_j;B,M_1,M_2)\Bigg]\\
&+\sum_{l=2}^{5}\Big(C_{2l-1}CA_{2l-1}(d_i,q_j,q_k;B,M_1,M_2)+C_{2l}DA_{2l}(d_i,q_j,q_k;B,M_1,M_2)\Big)\,,
\end{aligned}$$

where $q_k = d$, u or s for B_d, B^+ and B_s decays respectively and $q = u$, d, s and c. The second and the last line on the r.h.s. of eq. (28) can be readily found by following fig. 10. The relevant quark variables d_i and q_j in P_1 can be identified from the penguin insertion of Q_1 as seen on the top of fig. 10. The variable d_i denotes the quark line flowing into the penguin. The variable q_j denotes the quark line attached to d_i on its right hand side.

$$\begin{aligned}
P_2(d_i,q_j;B,M_1,M_2) &= C_1 CPE_1(c,q_j,d_i;B,M_1,M_2)+C_2 DPE_2(c,q_j,d_i;B,M_1,M_2) \qquad (29)\\
&+\sum_{l=2}^{5}\Big(C_{2l-1}DE_{2l-1}(q_j,q_j,d_i;B,M_1,M_2)+C_{2l}CE_{2l}(q_j,q_j,d_i;B,M_1,M_2)\Big)
\end{aligned}$$

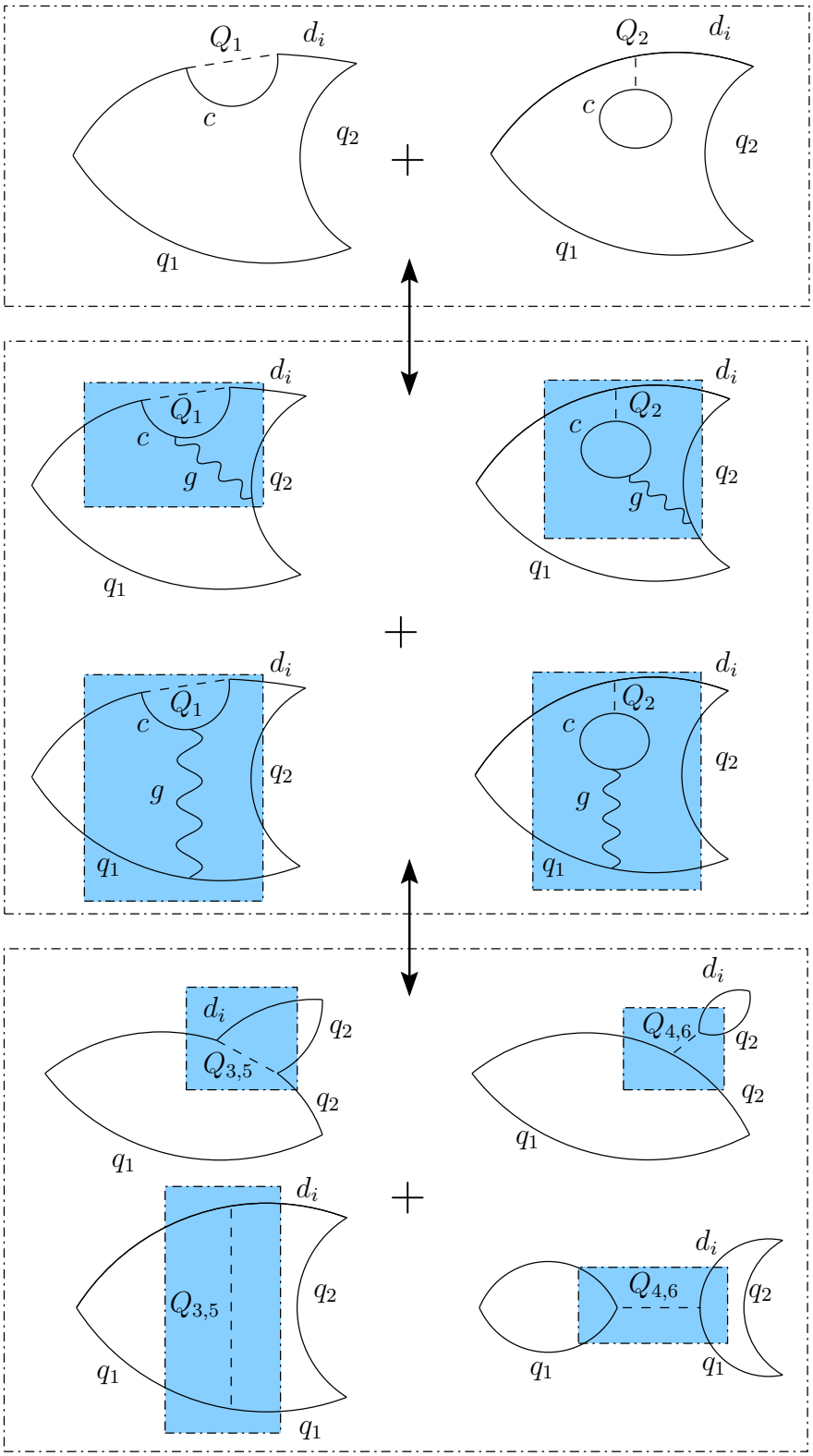

Figure 10: A diagrammatic representation of the correspondence between penguin-like contractions of current-current operators and insertions of penguin operators. See the text for details.

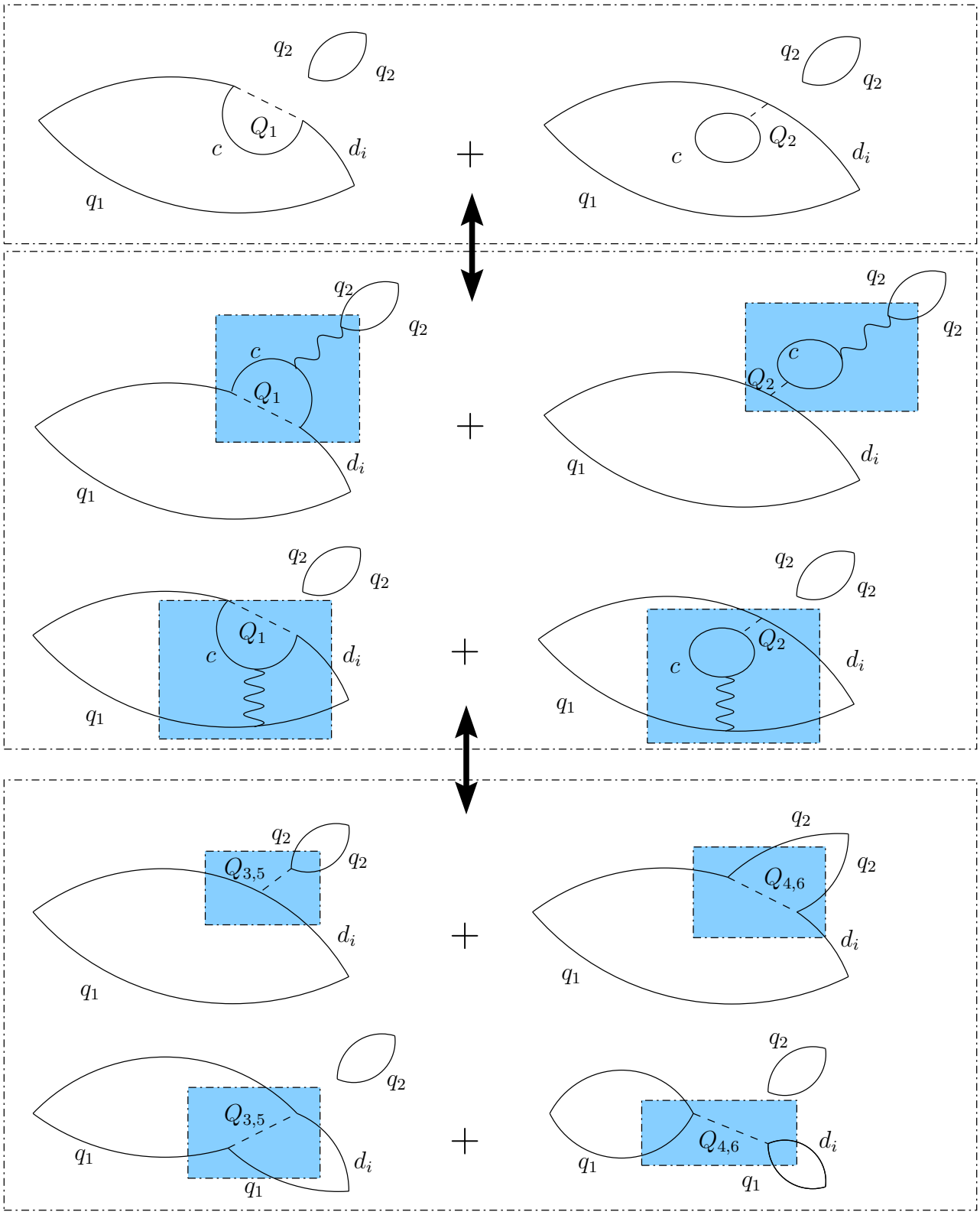

Figure 11: A diagrammatic representation of the correspondence between penguin-emission contractions of current-current operators and insertions of penguin operators. See the text for details.

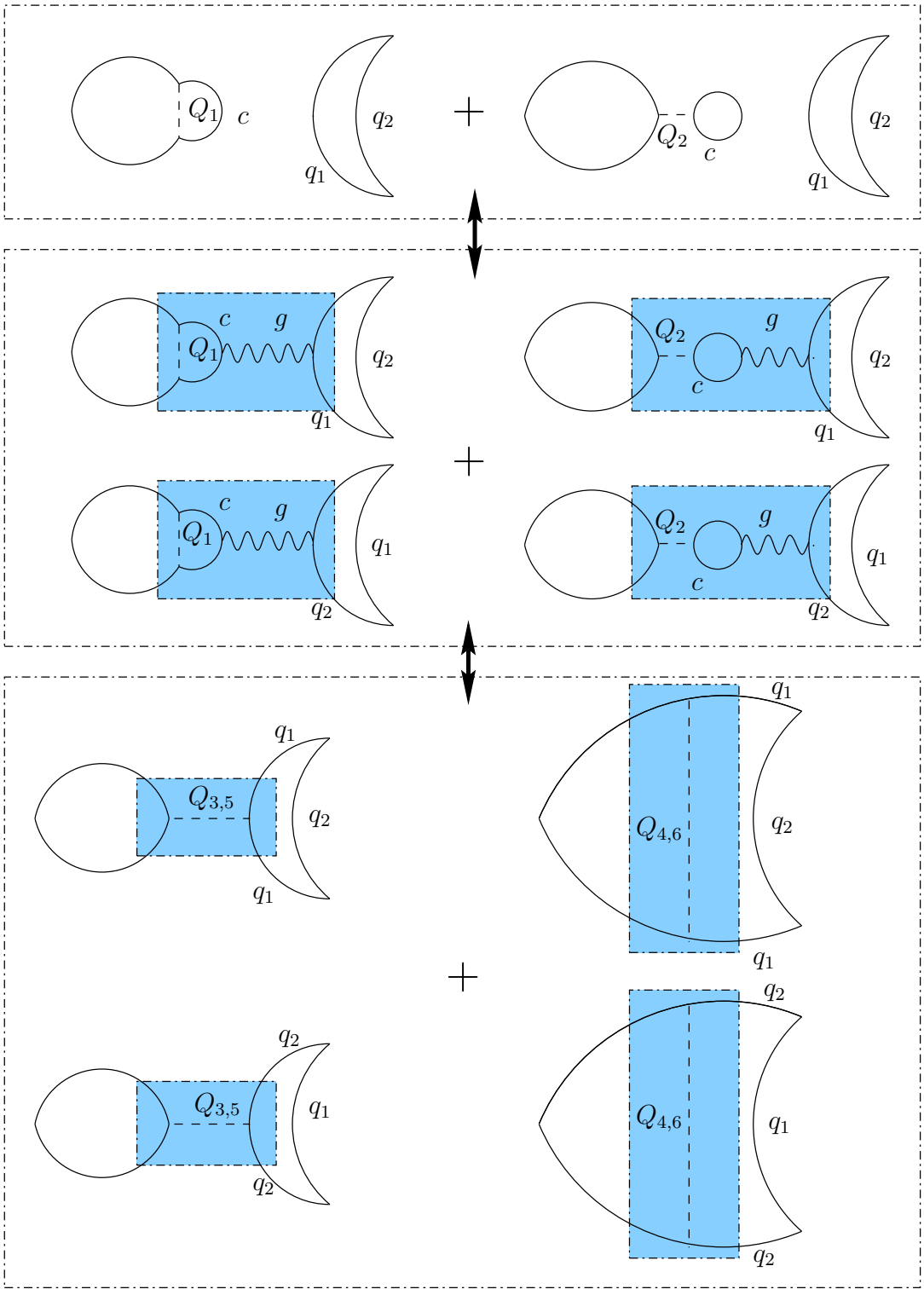

Figure 12: A diagrammatic representation of the correspondence between penguin-annihilation contractions of current-current operators and insertions of penguin operators. See the text for details.

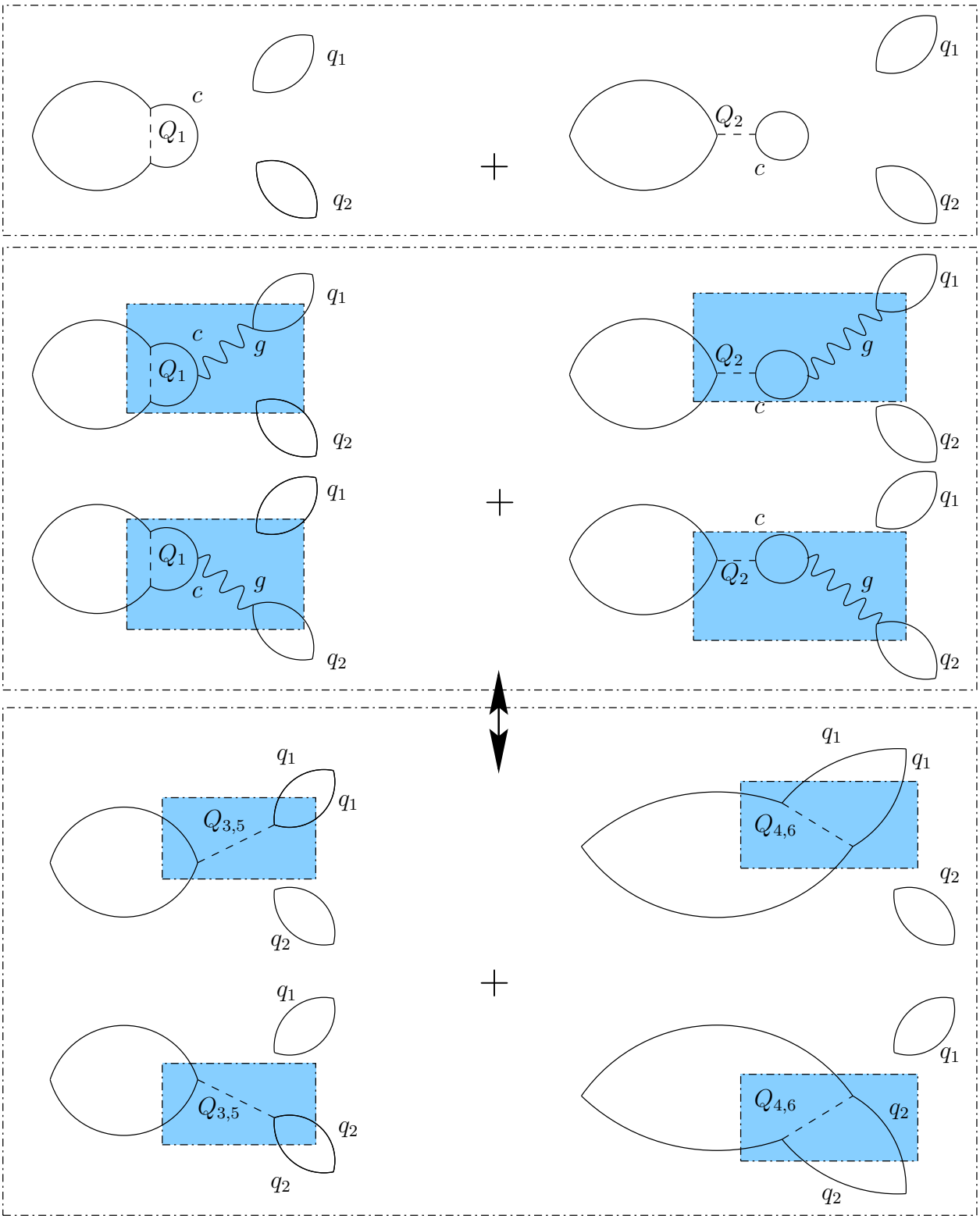

Figure 13: A diagrammatic representation of the correspondence between double-penguin-annihilation contractions of current-current operators and insertions of penguin operators. See the text for details.

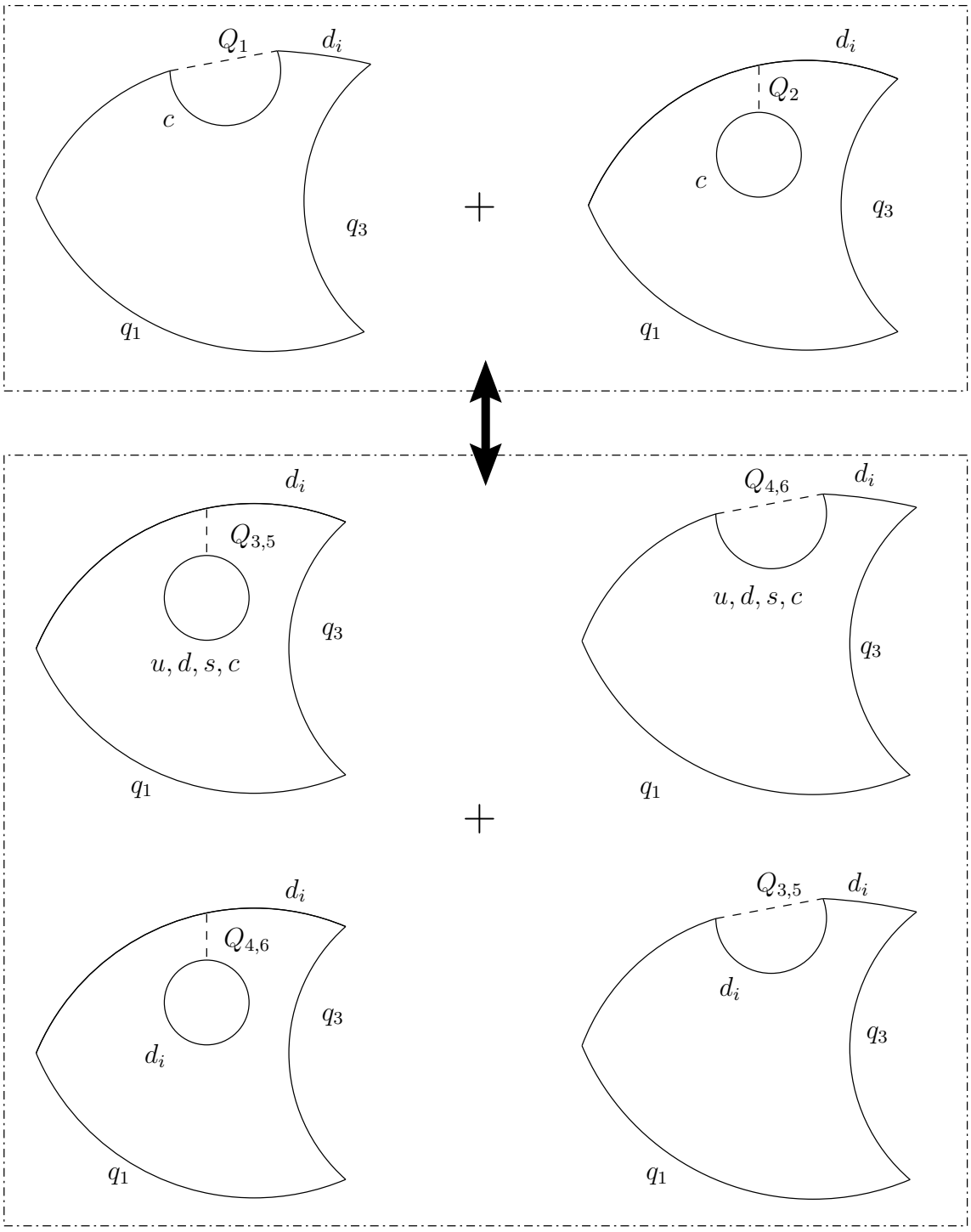

Figure 14: A diagrammatic representation of the rule to obtain contribution c). See the text for details.

$$
\begin{aligned}
&+ \sum_{l=2}^{5}\Big(C_{2l-1}\,CEA_{2l-1}(d_i,q_k,q_j;B,M_2,M_1)+C_{2l}\,DEA_{2l}(d_i,q_k,q_j;B,M_2,M_1)\Big)\\
&+ \sum_{l=2}^{5}\Bigg[\sum_q\Big(C_{2l-1}\,DPE_{2l-1}(q,q_j,d_i;B,M_1,M_2)+C_{2l}\,CPE_{2l}(q,q_j,d_i;B,M_1,M_2)\Big)\\
&\qquad +C_{2l-1}\,CPE_{2l-1}(d_i,q_j,d_i;B,M_1,M_2)+C_{2l}\,DPE_{2l}(d_i,q_j,d_i;B,M_1,M_2)\Bigg],
\end{aligned}
$$

where $q_k = d$, u or s for B_d, B^+ and B_s decays respectively. The second and the third line on the r.h.s. of eq. (29) can be found by following fig. 11. The relevant quark variables d_i and q_j in P_2 can be identified from the relevant penguin insertion of Q_1 as seen on the top of fig. 11. The variable d_i denotes the quark line flowing into the penguin. The variable q_j denotes the flavour in the neutral "blob" representing the meson $\bar{q}_j q_j$.

$$
\begin{aligned}
P_3(q_j,q_k;B,M_1,M_2) &= C_1\,CPA_1(c,q_j,q_k;B,M_1,M_2)+C_2\,DPA_2(c,q_j,q_k;B,M_1,M_2) \qquad (30)\\
&+ \sum_{l=2}^{5}\Big(C_{2l-1}\,DA_{2l-1}(q_k,q_j,q_k;B,M_1,M_2)+C_{2l}\,CA_{2l}(q_k,q_j,q_k;B,M_1,M_2)\Big)\\
&+ \sum_{l=2}^{5}\Big(C_{2l-1}\,DA_{2l-1}(q_j,q_k,q_j;B,M_2,M_1)+C_{2l}\,CA_{2l}(q_j,q_k,q_j;B,M_2,M_1)\Big)\\
&+ \sum_{l=2}^{5}\Bigg[\sum_q\Big(C_{2l-1}\,DPA_{2l-1}(q,q_j,q_k;B,M_1,M_2)+C_{2l}\,CPA_{2l}(q,q_j,q_k;B,M_1,M_2)\Big)\\
&\qquad +C_{2l-1}\,CPA_{2l-1}(d_i,q_j,q_k;B,M_1,M_2)+C_{2l}\,DPA_{2l}(d_i,q_j,q_k;B,M_1,M_2)\Bigg],
\end{aligned}
$$

where $d_i = d$ or s for B_d and B_s decays respectively (due to the flavour structure, P_3 cannot contribute to charged B decays). The second and third lines on the r.h.s. of eq. (30) can be found using fig. 12. The relevant quark variables q_j and q_k in P_3 can be identified from the relevant penguin insertion of Q_1 as seen on the top of fig. 12. The variable q_j denotes the external quark line in the right hand side of the diagram. The variable q_k denotes the internal quark line in this part of the diagram.

$$
\begin{aligned}
P_4(q_j,q_k;B,M_1,M_2) &= C_1\,\overline{CPA}_1(c,q_j,q_k;B,M_1,M_2)+C_2\,\overline{DPA}_2(c,q_j,q_k;B,M_1,M_2) \qquad (31)\\
&+ \sum_{l=2}^{5}\Big(C_{2l-1}\,DEA_{2l-1}(q_j,q_j,q_k;B,M_1,M_2)+C_{2l}\,CEA_{2l}(q_j,q_j,q_k;B,M_1,M_2)\Big)\\
&+ \sum_{l=2}^{5}\Big(C_{2l-1}\,DEA_{2l-1}(q_k,q_k,q_j;B,M_2,M_1)+C_{2l}\,CEA_{2l}(q_k,q_k,q_j;B,M_2,M_1)\Big)\\
&+ \sum_{l=2}^{5}\Bigg[\sum_q\Big(C_{2l-1}\,\overline{DPA}_{2l-1}(q,q_j,q_k;B,M_1,M_2)+C_{2l}\,\overline{CPA}_{2l}(q,q_j,q_k;B,M_1,M_2)\Big)\\
&\qquad +C_{2l-1}\,\overline{CPA}_{2l-1}(d_i,q_j,q_k;B,M_1,M_2)+C_{2l}\,\overline{DPA}_{2l}(d_i,q_j,q_k;B,M_1,M_2)\Bigg],
\end{aligned}
$$

where $d_i = d$ or s for B_d and B_s decays respectively (analogously to P_3, due to the flavour structure, P_4 cannot contribute to charged B decays). The second and third lines on the r.h.s. of eq. (31) can be found using fig. 13. The relevant quark variables q_j and q_k in P_4 can be identified from the relevant

penguin insertion of Q_1 as seen on the top of fig. 13. The variable q_j denotes the flavour in the upper neutral "blob" representing the meson $\bar{q}_j q_j$. The variable q_k denotes the corresponding flavour in the lower neutral meson $\bar{q}_k q_k$.

If factorization held, the penguin-type matrix elements would vanish and one would be left with the factorized emission and annihilation matrix elements of penguin operators.

5.5 The GIM-Penguin Parameters

The last four effective parameters are the GIM-penguin ones, $P_1^{\rm GIM}$, $P_2^{\rm GIM}$, $P_3^{\rm GIM}$ and $P_4^{\rm GIM}$, already introduced in eq. (15). Their explicit flavour structure is given as follows:

$$\begin{aligned}
P_1^{\rm GIM}(d_i,q_j;B,M_1,M_2) &= C_1\Big(CP_1(c,d_i,q_j;B,M_1,M_2)-CP_1(u,d_i,q_j;B,M_1,M_2)\Big) \\
&+ C_2\Big(DP_2(c,d_i,q_j;B,M_1,M_2)-DP_2(u,d_i,q_j;B,M_1,M_2)\Big), \\
P_2^{\rm GIM}(d_i,q_j;B,M_1,M_2) &= C_1\Big(CPE_1(c,q_j,d_i;B,M_1,M_2)-CPE_1(u,q_j,d_i;B,M_1,M_2)\Big) \\
&+ C_2\Big(DPE_2(c,q_j,d_i;B,M_1,M_2)-DPE_2(u,q_j,d_i;B,M_1,M_2)\Big), \\
P_3^{\rm GIM}(q_j,q_k;B,M_1,M_2) &= C_1\Big(CPA_1(c,q_j,q_k;B,M_1,M_2)-CPA_1(u,q_j,q_k;B,M_1,M_2)\Big) \\
&+ C_2\Big(DPA_2(c,q_j,q_k;B,M_1,M_2)-DPA_2(u,q_j,q_k;B,M_1,M_2)\Big), \\
P_4^{\rm GIM}(q_j,q_k;B,M_1,M_2) &= C_1\Big(\overline{CPA}_1(c,q_j,q_k;B,M_1,M_2)-\overline{CPA}_1(u,q_j,q_k;B,M_1,M_2)\Big) \\
&+ C_2\Big(\overline{DPA}_2(c,q_j,q_k;B,M_1,M_2)-\overline{DPA}_2(u,q_j,q_k;B,M_1,M_2)\Big).
\end{aligned} \tag{32}$$

6 Hierarchies

In the previous Sections we have introduced the effective scheme and scale independent parameters suitable for the description of two-body B decays, and we have discussed in detail their flavour structure. In this Section, we show, using the large N approximation, that a hierarchy is expected between the various parameters which we previously introduced.

Using the large N classification one has in units of $\sqrt{N}$ the following hierarchy for various topologies:

$$\begin{aligned}
DE,\, DA &: \mathcal{O}(1), \\
CE,\, CA,\, DEA,\, CP,\, DPA,\, DPE &: \mathcal{O}(1/N), \\
CEA,\, DP,\, CPA,\, CPE,\, \overline{DPA} &: \mathcal{O}(1/N^2), \\
\overline{CPA} &: \mathcal{O}(1/N^3).
\end{aligned} \tag{33}$$

On the other hand the Wilson coefficients C_{1-6} have in the strict $1/N$ classification the following dependence:

$$\begin{aligned}
C_1 &: \mathcal{O}(1), \\
C_2\,,\, C_4\,,\, C_6 &: \mathcal{O}(1/N), \\
C_3\,,\, C_5 &: \mathcal{O}(1/N^2).
\end{aligned} \tag{34}$$

The coefficients C_{7-10} are all $\mathcal{O}(\alpha)$ and consequently the large N classification of C_{7-10} with respect to C_{1-6} is not useful here. In discussing the $1/N$ hierarchy of the effective parameters we will therefore not include the electroweak penguin operators.

Two additional comments on (33) and (34) should be made. If there is an s-channel resonance, as in the case of annihilation contributions, there is an additional enhancement factor N as in the large N limit the width of a resonance behaves as $\Gamma \sim 1/N$. On the other hand annihilation is suppressed by other dynamical factors and it is justified to ignore this additional factor of N in the following discussion.

Concerning (34), the Wilson coefficients can be enhanced by large logarithms due to the renormalization group evolution from M_W down to m_b. Since $\ln M_W^2/m_b^2 \sim 6$, these logarithms may over-compensate the $1/N$ suppression. On the other hand as seen in (7) $C_1 > C_2 > C_{4,6} > C_{3,5}$. Thus except for C_2 being substantially higher than $C_{4,6}$ the hierarchy in (34) is roughly respected and we will consider it to be valid in the following discussion.

Using (33) and (34) we find the following large N classification of the effective parameters in units of $\sqrt{N}$:

$$\begin{aligned} E_1,\ A_1 &: \mathcal{O}(1), \\ E_2,\ A_2,\ EA_1,\ P_1,\ P_1^{\rm GIM} &: \mathcal{O}(1/N), \\ EA_2,\ P_2,\ P_3,\ P_2^{\rm GIM},\ P_3^{\rm GIM} &: \mathcal{O}(1/N^2), \\ P_4,\ P_4^{\rm GIM} &: \mathcal{O}(1/N^3). \end{aligned} \tag{35}$$

As one can see, within the large N classification the annihilation amplitude A_1 is expected to be larger than E_2, which contradicts the usual expectations. Future measurements of channels dominated by A_1 or E_2 will teach us whether this hierarchy is consistent with the data.

Next, the decay amplitudes are linear combinations of effective parameters multiplied by CKM factors. The hierarchy of the latter can be roughly described in terms of the Wolfenstein parameter $\lambda = |V_{us}| = 0.22$. In particular we have:

$$V_{us}V_{ub}^* = \mathcal{O}\left(\lambda^4\right), \quad V_{ts}V_{tb}^* = \mathcal{O}\left(\lambda^2\right), \quad V_{ud}V_{ub}^* = \mathcal{O}\left(\lambda^3\right), \quad V_{td}V_{tb}^* = \mathcal{O}\left(\lambda^3\right). \tag{36}$$

When calculating branching ratios one could for instance neglect $V_{us}V_{ub}^*$ with respect to $V_{ts}V_{tb}^*$ provided this is also supported by the hierarchy in (35). On the other hand when studying CP-asymmetries it is important to keep all CKM factors and we will do so in the following.

In tables 1–3 we collect a large number of two-body B_d, B^+ and B_s decays respectively. We list there the effective parameters contributing to each decay, the size of each parameter according to the large N classification and the order in λ of the CKM parameters multiplying it. These tables should be useful in identifying the most suitable decays for the determination of the effective parameters and for approximations which would reduce the number of parameters.

In the following Sections we will present explicit expressions for the amplitudes of the two-body B decays listed in tables 1–3. In order to simplify the presentation we will omit in Sections 7 and 8:

1. the contributions proportional to the parameters P_4 and $P_4^{\rm GIM}$;
2. the contributions which vanish in the $SU(2)$ limit, unless their neglect would make a CKM factor disappear from the amplitude.

The contributions omitted in Sections 7 and 8 are listed for completeness in Appendix A.

Channel	Cl.	E_1	E_2	EA_2	A_2	P_1	P_2	P_3	$P_1^{\rm GIM}$	$P_2^{\rm GIM}$	$P_3^{\rm GIM}$	P_4	$P_4^{\rm GIM}$
		1	$\frac{1}{N}$	$\frac{1}{N^2}$	$\frac{1}{N}$	$\frac{1}{N}$	$\frac{1}{N^2}$	$\frac{1}{N^2}$	$\frac{1}{N}$	$\frac{1}{N^2}$	$\frac{1}{N^2}$	$\frac{1}{N^3}$	$\frac{1}{N^3}$
$B_d \to D^-\pi^+$	**A**	λ^2	–	–	λ^2	–	–	–	–	–	–	–	–
$B_d \to \bar{D}^0\pi^0$	**A**	–	λ^2	$[\lambda^2]$	λ^2	–	–	–	–	–	–	–	–
$B_d \to D^-K^+$	**B**	λ^3	–	–	–	–	–	–	–	–	–	–	–
$B_d \to \bar{D}^0K^0$	**B**	–	λ^3	–	–	–	–	–	–	–	–	–	–
$B_d \to D^0K^0$	**B**	–	λ^3	–	–	–	–	–	–	–	–	–	–
$B_d \to D_s^+\pi^-$	**B**	λ^3	–	–	–	–	–	–	–	–	–	–	–
$B_d \to J/\psi K^0$	**C**	–	λ^2	–	–	–	λ^2	–	–	λ^4	–	–	–
$B_d \to D_s^+D^-$	**C**	λ^2	–	–	–	λ^2	–	–	λ^4	–	–	–	–
$B_d \to \pi^0\pi^0$	**D**	–	λ^3	$[\lambda^3]$	λ^3	λ^3	$[\lambda^3]$	λ^3	λ^3	$[\lambda^3]$	λ^3	$[\lambda^3]$	$[\lambda^3]$
$B_d \to \pi^+\pi^-$	**D**	λ^3	–	–	λ^3	λ^3	–	λ^3	λ^3	–	λ^3	–	–
$B_d \to D^+D^-$	**D**	λ^3	–	–	λ^3	λ^3	–	λ^3	λ^3	–	λ^3	–	–
$B_d \to \pi^0 J/\psi$	**D**	–	λ^3	λ^3	–	–	λ^3	–	–	λ^3	–	$[\lambda^3]$	$[\lambda^3]$
$B_d \to K^+\pi^-$	**E**	λ^4	–	–	–	λ^2	–	–	λ^4	–	–	–	–
$B_d \to K^0\pi^0$	**E**	–	λ^4	–	–	λ^2	$[\lambda^2]$	–	λ^4	$[\lambda^4]$	–	–	–
$B_d \to K^0\phi$	**E**	–	–	–	–	λ^2	λ^2	–	λ^4	λ^4	–	–	–
$B_d \to K^0\bar{K}^0$	**F**	–	–	–	–	λ^3	–	λ^3	λ^3	–	λ^3	–	–
$B_d \to \phi\pi^0$	**F**	–	–	λ^3	–	–	λ^3	–	–	λ^3	–	$[\lambda^3]$	$[\lambda^3]$
$B_d \to \phi\phi$	**F**	–	–	–	–	–	–	λ^3	–	–	λ^3	λ^3	λ^3
$B_d \to D_s^-K^+$	**G**	–	–	–	λ^2	–	–	–	–	–	–	–	–
$B_d \to \bar{D}^0 J/\psi$	**G**	–	–	λ^2	λ^2	–	–	–	–	–	–	–	–
$B_d \to \bar{D}^0\phi$	**G**	–	–	λ^2	–	–	–	–	–	–	–	–	–
$B_d \to K^+K^-$	**G**	–	–	–	λ^3	–	–	λ^3	–	–	λ^3	–	–
$B_d \to D_s^+D_s^-$	**G**	–	–	–	λ^3	–	–	λ^3	–	–	λ^3	–	–
$B_d \to D^0\bar{D}^0$	**G**	–	–	–	λ^3	–	–	λ^3	–	–	λ^3	–	–

Table 1: Summary of the classification of two-body B_d decays discussed in Section 7. For each channel, the order in the Wolfenstein parameter λ of the relevant contributions is given. The contributions in squared brackets are of order α and they vanish in the limit of $SU(2)$ symmetry (see Appendix A); these contributions, together with the ones in the last two columns, have been neglected in the analysis of Section 7 wherever possible.

Channel	Class	E_1 1	E_2 $\frac{1}{N}$	A_1 1	EA_1 $\frac{1}{N}$	P_1 $\frac{1}{N}$	P_2 $\frac{1}{N^2}$	$P_1^{\rm GIM}$ $\frac{1}{N}$	$P_2^{\rm GIM}$ $\frac{1}{N^2}$
$B^+ \to \bar{D}^0\pi^+$	**A**	λ^2	λ^2	–	–	–	–	–	–
$B^+ \to \bar{D}^0K^+$	**B**	λ^3	λ^3	–	–	–	–	–	–
$B^+ \to D^0K^+$	**B**	–	λ^3	λ^3	–	–	–	–	–
$B^+ \to D_s^+\pi^0$	**B**	λ^3	–	–	$[\lambda^3]$	–	–	–	–
$B^+ \to J/\psi K^+$	**C**	–	λ^2	–	λ^4	–	λ^2	–	λ^4
$B^+ \to D_s^+\bar{D}^0$	**C**	λ^2	–	λ^4	–	λ^2	–	λ^4	–
$B^+ \to \pi^+\pi^0$	**D**	λ^3	λ^3	$[\lambda^3]$	$[\lambda^3]$	$[\lambda^3]$	$[\lambda^3]$	$[\lambda^3]$	$[\lambda^3]$
$B^+ \to K^+\bar{K}^0$	**D**	–	–	λ^3	–	λ^3	–	λ^3	–
$B^+ \to \pi^+J/\psi$	**D**	–	λ^3	–	λ^3	–	λ^3	–	λ^3
$B^+ \to D^+\bar{D}^0$	**D**	λ^3	–	λ^3	–	λ^3	–	λ^3	–
$B^+ \to K^0\pi^+$	**E**	–	–	λ^4	–	λ^2	–	λ^4	–
$B^+ \to K^+\pi^0$	**E**	λ^4	λ^4	λ^4	$[\lambda^4]$	λ^2	$[\lambda^2]$	λ^4	$[\lambda^4]$
$B^+ \to K^+\phi$	**E**	–	–	λ^4	λ^4	λ^2	λ^2	λ^4	λ^4
$B^+ \to \phi\pi^+$	**F**	–	–	–	λ^3	–	λ^3	–	λ^3
$B^+ \to D^+K^0$	**G**	–	–	λ^3	–	–	–	–	–
$B^+ \to D_s^+\phi$	**G**	–	–	λ^3	λ^3	–	–	–	–
$B^+ \to D_s^+J/\psi$	**G**	–	–	λ^3	λ^3	–	–	–	–

Table 2: Summary of the classification of two-body B^+ decays discussed in Section 7. For each channel, the order in the Wolfenstein parameter λ of the relevant contributions is given. The contributions in squared brackets are of order α and they vanish in the limit of $SU(2)$ symmetry (see Appendix A); they have been neglected in the analysis of Section 7 wherever possible.

Channel	Cl.	E_1 1	E_2 $\frac{1}{N}$	EA_2 $\frac{1}{N^2}$	A_2 $\frac{1}{N}$	P_1 $\frac{1}{N}$	P_2 $\frac{1}{N^2}$	P_3 $\frac{1}{N^2}$	$P_1^{\rm GIM}$ $\frac{1}{N}$	$P_2^{\rm GIM}$ $\frac{1}{N^2}$	$P_3^{\rm GIM}$ $\frac{1}{N^2}$	P_4 $\frac{1}{N^3}$	$P_4^{\rm GIM}$ $\frac{1}{N^3}$
$B_s \to D_s^- \pi^+$	**A**	λ^2	–	–	–	–	–	–	–	–	–	–	–
$B_s \to \bar{D}^0 \bar{K}^0$	**A**	–	λ^2	–	–	–	–	–	–	–	–	–	–
$B_s \to D_s^- K^+$	**B**	λ^3	–	–	λ^3	–	–	–	–	–	–	–	–
$B_s \to D_s^+ K^-$	**B**	λ^3	–	–	λ^3	–	–	–	–	–	–	–	–
$B_s \to \bar{D}^0 \phi$	**B**	–	λ^3	λ^3	–	–	–	–	–	–	–	–	–
$B_s \to D^0 \phi$	**B**	–	λ^3	λ^3	–	–	–	–	–	–	–	–	–
$B_s \to D^+ K^-$	**B**	λ^4	–	–	–	–	–	–	–	–	–	–	–
$B_s \to D^0 \bar{K}^0$	**B**	–	λ^4	–	–	–	–	–	–	–	–	–	–
$B_s \to \phi \pi^0$	**B**	–	λ^4	λ^4	–	–	$[\lambda^2]$	–	–	$[\lambda^4]$	–	$[\lambda^2]$	$[\lambda^4]$
$B_s \to J/\psi \phi$	**C**	–	λ^2	λ^2	–	–	λ^2	–	–	λ^4	–	λ^2	λ^4
$B_s \to D_s^+ D_s^-$	**C**	λ^2	–	–	λ^2	λ^2	–	λ^2	λ^4	–	λ^4	–	–
$B_s \to \pi^0 \bar{K}^0$	**D**	–	λ^3	–	–	λ^3	$[\lambda^3]$	–	λ^3	$[\lambda^3]$	–	–	–
$B_s \to \pi^+ K^-$	**D**	λ^3	–	–	–	λ^3	–	–	λ^3	–	–	–	–
$B_s \to J/\psi \bar{K}^0$	**D**	–	λ^3	–	–	–	λ^3	–	–	λ^3	–	–	–
$B_s \to D^+ D_s^-$	**D**	λ^3	–	–	–	λ^3	–	–	λ^3	–	–	–	–
$B_s \to K^0 \bar{K}^0$	**E**	–	–	–	–	λ^2	–	λ^2	λ^4	–	λ^4	–	–
$B_s \to \phi \phi$	**E**	–	–	–	–	λ^2	λ^2	λ^2	λ^4	λ^4	λ^4	λ^2	λ^4
$B_s \to \pi^+ \pi^-$	**E**	–	–	–	λ^4	–	–	λ^2	–	–	λ^4	–	–
$B_s \to \pi^0 \pi^0$	**E**	–	–	$[\lambda^4]$	λ^4	–	–	λ^2	–	–	λ^4	$[\lambda^2]$	$[\lambda^4]$
$B_s \to K^+ K^-$	**E**	λ^4	–	–	λ^4	λ^2	–	λ^2	λ^4	–	λ^4	–	–
$B_s \to \bar{K}^0 \phi$	**F**	–	–	–	–	λ^3	λ^3	–	λ^3	λ^3	–	–	–
$B_s \to D^{-}_{0} \overset{(-)}{D}{}^{+}_{0}$	**G**	–	–	–	λ^2	–	–	λ^2	–	–	λ^4	–	–
$B_s \to \pi^0 J/\psi$	**G**	–	–	$[\lambda^2]$-λ^4	–	–	–	–	–	–	–	$[\lambda^2]$	$[\lambda^4]$
$B_s \to \pi^{\pm} D^{\mp}$	**G**	–	–	–	λ^3	–	–	–	–	–	–	–	–
$B_s \to \pi^0 \overset{(-)}{D}{}^{0}$	**G**	–	–	$[\lambda^3]$	λ^3	–	–	–	–	–	–	–	–
$B_s \to J/\psi D^0$	**G**	–	–	λ^3	λ^3	–	–	–	–	–	–	–	–
$B_s \to J/\psi \bar{D}^0$	**G**	–	–	λ^3	λ^3	–	–	–	–	–	–	–	–

Table 3: Summary of the classification of two-body B_s decays discussed in Section 8. For each channel, the order in the Wolfenstein parameter λ of the relevant contributions is given. The contributions in squared brackets are of order α and they vanish in the limit of $SU(2)$ symmetry (see Appendix A); they have been neglected in the analysis of Section 8, together with the contributions in the last two columns, wherever possible.

7 Classification of Two-Body B Decays

Using the effective parameters defined above, we can classify the two-body B decay channels according to the effective parameters entering in the decay amplitude. This classification enables us to identify subsets of channels that, when measured, would allow us to directly extract the effective parameters previously defined, making no assumption about non-factorizable contributions and rescattering. We postpone the discussion of channels with η and η' in the final state to a future publication.

As we discussed in the previous Section, we neglect here, wherever it is possible, contributions proportional to the parameters P_4 and $P_4^{\rm GIM}$, and contributions that vanish in the $SU(2)$ symmetric limit. The expressions for the neglected terms, denoted in this Section by $\Delta\mathcal{A}$, can be found in Appendix A.

We use the following conventions for the flavour content of mesons:

$$\begin{array}{lllllll} B^+ = \bar{b}u, & B_d = \bar{b}d, & B_s = \bar{b}s, & \pi^+ = \bar{d}u, & \pi^0 = \frac{1}{\sqrt{2}}\left(\bar{d}d - \bar{u}u\right), & \pi^- = -\bar{u}d, & \\ K^+ = \bar{s}u, & K^0 = \bar{s}d, & \bar{K}^0 = \bar{d}s, & K^- = -\bar{u}s, & D_s^+ = \bar{s}c, & D_s^- = \bar{c}s, & \\ D^+ = \bar{d}c, & D^- = \bar{c}d, & D^0 = -\bar{u}c, & \bar{D}^0 = \bar{c}u, & \phi = \bar{s}s, & J/\psi = \bar{c}c, & \end{array} \tag{37}$$

which agree with refs. [18].

Class A decays

Class **A** decays are CKM-allowed penguin-free decay channels. These are particularly interesting since they would allow us to extract E_1 and E_2. A typical example is given by $B \to D\pi$ decays. We have (here and in the following we give results in units of $G_F/\sqrt{2}$):

$$\begin{aligned} \mathcal{A}(B_d \to D^-\pi^+) &= V_{ud}V_{cb}^*\Big(E_1(d,u,c;B_d,\pi^+,D^-) + A_2(c,d,u;B_d,D^-,\pi^+)\Big)\,; \\ \mathcal{A}(B_d \to \bar{D}^0\pi^0) &= \frac{V_{ud}V_{cb}^*}{\sqrt{2}}\Big(E_2(c,u,d;B_d,\bar{D}^0,\pi^0) - A_2(c,u,u;B_d,\bar{D}^0,\pi^0)\Big) + \Delta\mathcal{A}(B_d \to \bar{D}^0\pi^0)\,; \\ \mathcal{A}(B^+ \to \bar{D}^0\pi^+) &= V_{ud}V_{cb}^*\Big(E_1(d,u,c;B^+,\pi^+,\bar{D}^0) + E_2(c,u,d;B^+,\bar{D}^0,\pi^+)\Big)\,. \end{aligned} \tag{38}$$

Other channels in class **A** are obtained by replacing D by D^* and/or π by ρ.

Class B decays

These are penguin-free CKM-suppressed decay channels. A typical example of class **B** channels is given by $B \to DK$ decays. We have:

$$\begin{aligned} \mathcal{A}(B_d \to D^-K^+) &= V_{us}V_{cb}^*\,E_1(s,u,c;B_d,K^+,D^-)\,; \\ \mathcal{A}(B_d \to \bar{D}^0K^0) &= V_{us}V_{cb}^*\,E_2(c,u,s;B_d,\bar{D}^0,K^0)\,; \\ \mathcal{A}(B^+ \to \bar{D}^0K^+) &= V_{us}V_{cb}^*\Big(E_1(s,u,c;B^+,K^+,\bar{D}^0) + E_2(c,u,s;B^+,\bar{D}^0,K^+)\Big)\,. \end{aligned} \tag{39}$$

The above channels are very interesting since they are also annihilation-free and therefore would provide us with a cleaner measurement of emission matrix elements with respect to class **A** decays. The same holds for the analogous channels with vector mesons.

Other interesting class **B** decay channels are the following:

$$\begin{aligned}
\mathcal{A}(B_d \to D^0 K^0) &= -V_{cs}V_{ub}^*\, E_2(u,c,s;B_d,D^0,K^0)\,,\\
\mathcal{A}(B^+ \to D^0 K^+) &= -V_{cs}V_{ub}^*\Big(E_2(u,c,s;B^+,D^0,K^+) + A_1(s,u,c;B^+,K^+,D^0)\Big)\,,\\
\mathcal{A}(B_d \to D_s^+ \pi^-) &= -V_{cs}V_{ub}^*\, E_1(s,c,u;B_d,D_s^+,\pi^-)\,,\\
\mathcal{A}(B^+ \to D_s^+ \pi^0) &= -\frac{V_{cs}V_{ub}^*}{\sqrt{2}} E_1(s,c,u;B^+,D_s^+,\pi^0) + \Delta\mathcal{A}(B^+ \to D_s^+\pi^0)\,,
\end{aligned} \tag{40}$$

plus the corresponding ones with vector mesons.

Class C decays

Class **C** decays are CKM-allowed channels in which penguin contributions are present (but not dominant). Here are some typical examples:

$$\begin{aligned}
\mathcal{A}(B_d \to J/\psi K^0) &= V_{cs}V_{cb}^*\, E_2(c,c,s;B_d,J/\psi,K^0) - V_{ts}V_{tb}^*\, P_2(s,c;B_d,J/\psi,K^0) -\\
&\quad V_{us}V_{ub}^* P_2^{\rm GIM}(s,c;B_d,J/\psi,K^0)\,;\\
\mathcal{A}(B^+ \to J/\psi K^+) &= V_{cs}V_{cb}^*\, E_2(c,c,s;B^+,J/\psi,K^+) - V_{ts}V_{tb}^*\, P_2(s,c;B^+,J/\psi,K^+) -\\
&\quad V_{us}V_{ub}^*\Big(P_2^{\rm GIM}(s,c;B^+,J/\psi,K^+) - EA_1(s,u,c;B^+,K^+,J/\psi)\Big)\,;\\
\mathcal{A}(B_d \to D_s^+ D^-) &= V_{cs}V_{cb}^*\, E_1(s,c,c;B_d,D_s^+,D^-) - V_{ts}V_{tb}^*\, P_1(s,c;B_d,D_s^+,D^-) -\\
&\quad V_{us}V_{ub}^*\, P_1^{\rm GIM}(s,c;B_d,D_s^+,D^-)\,;\\
\mathcal{A}(B^+ \to D_s^+ \bar{D}^0) &= V_{cs}V_{cb}^*\, E_1(s,c,c;B^+,D_s^+,\bar{D}^0) - V_{ts}V_{tb}^*\, P_1(s,c;B^+,D_s^+,\bar{D}^0) +\\
&\quad V_{us}V_{ub}^*\Big(A_1(s,c,u;B^+,D_s^+,\bar{D}^0) - P_1^{\rm GIM}(s,c;B^+,D_s^+,\bar{D}^0)\Big)\,.
\end{aligned} \tag{41}$$

Class D decays

Class **D** decays are CKM-suppressed decays in which penguin contributions are present. Well-known examples of this kind are $B \to \pi\pi$ decays:

$$\begin{aligned}
\sqrt{2}\mathcal{A}(B_d \to \pi^0\pi^0) = &- V_{ud}V_{ub}^*\Big(E_2(u,u,d;B_d,\pi^0,\pi^0) - A_2(u,u,u;B_d,\pi^0,\pi^0) + P_1^{\rm GIM}(d,d;B_d,\pi^0,\pi^0)\\
&\qquad + \frac{1}{2}P_3^{\rm GIM}(d,d;B_d,\pi^0,\pi^0) + \frac{1}{2}P_3^{\rm GIM}(u,u;B_d,\pi^0,\pi^0)\Big)\\
&- V_{td}V_{tb}^*\Big(P_1(d,d;B_d,\pi^0,\pi^0) + \frac{1}{2}P_3(d,d;B_d,\pi^0,\pi^0) + \frac{1}{2}P_3(u,u;B_d,\pi^0,\pi^0)\Big)\\
&+ \Delta\mathcal{A}(B_d \to \pi^0\pi^0)\,;\\
\mathcal{A}(B_d \to \pi^+\pi^-) = &- V_{ud}V_{ub}^*\Big(E_1(d,u,u;B_d,\pi^+,\pi^-) + A_2(u,d,u;B_d,\pi^-,\pi^+) -\\
&\qquad P_1^{\rm GIM}(d,u;B_d,\pi^+,\pi^-) - P_3^{\rm GIM}(u,d;B_d,\pi^+,\pi^-)\Big)\\
&+ V_{td}V_{tb}^*\Big(P_1(d,u;B_d,\pi^+,\pi^-) + P_3(u,d;B_d,\pi^+,\pi^-)\Big)\\
\mathcal{A}(B^+ \to \pi^+\pi^0) = &- \frac{V_{ud}V_{ub}^*}{\sqrt{2}}\Big(E_1(d,u,u;B^+,\pi^+,\pi^0) + E_2(u,u,d;B^+,\pi^0,\pi^+)\Big)\\
&- \frac{V_{td}V_{tb}^*}{\sqrt{2}}\Bigg(\Big[P_1(d,d;B^+,\pi^0,\pi^+) - P_1(d,u;B^+,\pi^+,\pi^0)\Big] +
\end{aligned}$$

$$\Big[P_2(d,d;B^+,\pi^0,\pi^+) - P_2(d,u;B^+,\pi^0,\pi^+)\Big]\Big)$$
$$+ \quad \Delta\mathcal{A}(B^+\to\pi^+\pi^0)\,, \tag{42}$$

where the quantities in square brackets in $\mathcal{A}(B^+\to\pi^+\pi^0)$ vanish in the limit of exact $SU(2)$ symmetry.

The presence of many different contributions with different weak phases and potentially different strong phases implies that it will be very difficult to extract $\sin 2\alpha$ from the measurement of the asymmetry in $B_d\to\pi^+\pi^-$ [26, 31].

Other channels in this class are the following:

$$\begin{aligned}
\mathcal{A}(B_d\to\pi^0 J/\psi) = &+ \frac{V_{cd}V_{cb}^*}{\sqrt{2}}E_2(c,c,d;B_d,J/\psi,\pi^0) - \frac{V_{td}V_{tb}^*}{\sqrt{2}}P_2(d,c;B_d,J/\psi,\pi^0)\\
&- \frac{V_{ud}V_{ub}^*}{\sqrt{2}}\Big(P_2^{\rm GIM}(d,c;B_d,J/\psi,\pi^0) - EA_2(u,u,c;B_d,\pi^0,J/\psi)\Big)\\
&+ \Delta\mathcal{A}(B_d\to\pi^0 J/\psi)\,;\\
\mathcal{A}(B_d\to D^+D^-) = &+ V_{cd}V_{cb}^*\Big(E_1(d,c,c;B_d,D^+,D^-) + A_2(c,d,c;B_d,D^-,D^+)\Big)\\
&- V_{ud}V_{ub}^*\Big(P_1^{\rm GIM}(d,c;B_d,D^+,D^-) + P_3^{\rm GIM}(d,c;B_d,D^-,D^+)\Big)\\
&- V_{td}V_{tb}^*\Big(P_1(d,c;B_d,D^+,D^-) + P_3(d,c;B_d,D^-,D^+)\Big)\,;\\
\mathcal{A}(B^+\to K^+\bar K^0) = &+ V_{ud}V_{ub}^*\Big(A_1(d,s,u;B^+,\bar K^0,K^+) - P_1^{\rm GIM}(d,s;B^+,\bar K^0,K^+)\Big)\\
&- V_{td}V_{tb}^*\,P_1(d,s;B^+,\bar K^0,K^+)\,;\\
\mathcal{A}(B^+\to\pi^+ J/\psi) = &+ V_{cd}V_{cb}^*\,E_2(c,c,d;B^+,J/\psi,\pi^+) - V_{td}V_{tb}^*\,P_2(d,c;B^+,J/\psi,\pi^+)\\
&- V_{ud}V_{ub}^*\Big(P_2^{\rm GIM}(d,c;B^+,J/\psi,\pi^+) - EA_1(d,u,c;B^+,\pi^+,J/\psi)\Big)\,;\\
\mathcal{A}(B^+\to D^+\bar D^0) = &+ V_{cd}V_{cb}^*\,E_1(d,c,c;B^+,D^+,\bar D^0) - V_{td}V_{tb}^*\,P_1(d,c;B^+,D^+,\bar D^0)\\
&+ V_{ud}V_{ub}^*\Big(A_1(d,c,u;B^+,D^+,\bar D^0) - P_1^{\rm GIM}(d,c;B^+,D^+,\bar D^0)\Big)\,,
\end{aligned} \tag{43}$$

and the corresponding channels with vector mesons replacing the pseudoscalars.

Class E decays

This very interesting class consists of (charming) penguin dominated channels. These decays would be doubly CKM suppressed if there were no penguins; since the penguin contributions are instead CKM allowed, they are expected to dominate the decay amplitude.

These modes have recently received a lot of attention after the observation at CLEO of $B\to K\pi$ decays [32]. As an example, we write down here the expression for these measured channels:

$$\begin{aligned}
\mathcal{A}(B_d\to K^+\pi^-) = &- V_{us}V_{ub}^*\Big(E_1(s,u,u;B_d,K^+,\pi^-) - P_1^{\rm GIM}(s,u;B_d,K^+,\pi^-)\Big)\\
&+ V_{ts}V_{tb}^*\,P_1(s,u;B_d,K^+,\pi^-)\,;\\
\mathcal{A}(B^+\to K^+\pi^0) = &- \frac{V_{us}V_{ub}^*}{\sqrt{2}}\Big(E_1(s,u,u;B^+,K^+,\pi^0) + E_2(u,u,s;B^+,\pi^0,K^+) -\\
&\qquad P_1^{\rm GIM}(s,u;B^+,K^+,\pi^0) + A_1(s,u,u;B^+,K^+,\pi^0)\Big)\\
&+ \frac{V_{ts}V_{tb}^*}{\sqrt{2}}P_1(s,u;B^+,K^+,\pi^0) + \Delta\mathcal{A}(B^+\to K^+\pi^0)\,;
\end{aligned}$$

$$\begin{aligned}
\mathcal{A}(B^+\to K^0\pi^+) = &+ V_{us}V_{ub}^*\Big(A_1(s,d,u;B^+,K^0,\pi^+) - P_1^{\rm GIM}(s,d;B^+,K^0,\pi^+)\Big)\\
&- V_{ts}V_{tb}^*\,P_1(s,d;B^+,K^0,\pi^+)\,. \qquad (44)
\end{aligned}$$

Other modes in this class are the following ones:

$$\begin{aligned}
\mathcal{A}(B_d\to K^0\pi^0) = &- \frac{V_{us}V_{ub}^*}{\sqrt{2}}\Big(E_2(u,u,s;B_d,\pi^0,K^0) + P_1^{\rm GIM}(s,d;B_d,K^0,\pi^0)\Big)\\
&- \frac{V_{ts}V_{tb}^*}{\sqrt{2}}P_1(s,d;B_d,K^0,\pi^0) + \Delta\mathcal{A}(B_d\to K^0\pi^0)\,;\\
\mathcal{A}(B_d\to K^0\phi) = &- V_{us}V_{ub}^*\Big(P_1^{\rm GIM}(s,s;B_d,\phi,K^0) + P_2^{\rm GIM}(s,s;B_d,\phi,K^0)\Big)\\
&- V_{ts}V_{tb}^*\Big(P_1(s,s;B_d,\phi,K^0) + P_2(s,s;B_d,\phi,K^0)\Big)\,;\\
\mathcal{A}(B^+\to K^+\phi) = &- V_{us}V_{ub}^*\Big(P_1^{\rm GIM}(s,s;B^+,\phi,K^+) + P_2^{\rm GIM}(s,s;B^+,\phi,K^+) -\\
&\qquad A_1(s,s,u;B^+,\phi,K^+) - EA_1(s,u,s;B^+,K^+,\phi)\Big)\\
&- V_{ts}V_{tb}^*\Big(P_1(s,s;B^+,\phi,K^+) + P_2(s,s;B^+,\phi,K^+)\Big)\,. \qquad (45)
\end{aligned}$$

Class F decays

These are CKM-suppressed pure penguin decays. Observation of these channels would also give us a measurement of penguin contributions. As an example, we write down the amplitudes for $B\to K^0\bar{K}^0$, $B\to\phi\pi$ and $B\to\phi\phi$ decays:

$$\begin{aligned}
\mathcal{A}(B_d\to K^0\bar{K}^0) = &- V_{ud}V_{ub}^*\Big(P_1^{\rm GIM}(d,s;B_d,\bar{K}^0,K^0) + P_3^{\rm GIM}(d,s;B_d,K^0,\bar{K}^0)\Big)\\
&- V_{td}V_{tb}^*\Big(P_1(d,s;B_d,\bar{K}^0,K^0) + P_3(d,s;B_d,K^0,\bar{K}^0)\Big)\,;\\
\mathcal{A}(B_d\to\phi\pi^0) = &- \frac{V_{ud}V_{ub}^*}{\sqrt{2}}\Big(P_2^{\rm GIM}(d,s;B_d,\phi,\pi^0) + EA_2(u,u,s;B_d,\pi^0,\phi)\Big)\\
&- \frac{V_{td}V_{tb}^*}{\sqrt{2}}P_2(d,s;B_d,\phi,\pi^0) + \Delta\mathcal{A}(B_d\to\phi\pi^0)\,;\\
\mathcal{A}(B^+\to\phi\pi^+) = &- V_{ud}V_{ub}^*\Big(P_2^{\rm GIM}(d,s;B^+,\phi,\pi^+) - EA_1(d,u,s;B^+,\pi^+,\phi)\Big)\\
&- V_{td}V_{tb}^*\,P_2(d,s;B^+,\phi,\pi^+)\,;\\
\sqrt{2}\mathcal{A}(B_d\to\phi\phi) = &- V_{ud}V_{ub}^*P_3^{\rm GIM}(s,s;B_d,\phi,\phi)\Big) - V_{td}V_{tb}^*P_3(s,s;B_d,\phi,\phi) + \Delta\mathcal{A}(B_d\to\phi\phi)\,. \qquad (46)
\end{aligned}$$

Class G decays

These decays proceed only via annihilations: a measurement of these channels would provide us with a direct determination of annihilation amplitudes.

The best examples of class **G** decays are these CKM-allowed channels:

$$\begin{aligned}
\mathcal{A}(B_d\to D_s^-K^+) &= V_{ud}V_{cb}^*\,A_2(c,s,u;B_d,D_s^-,K^+)\,;\\
\mathcal{A}(B_d\to\bar{D}^0J/\psi) &= V_{ud}V_{cb}^*\Big(A_2(c,c,u;B_d,J/\psi,\bar{D}^0) + EA_2(c,u,c;B_d,\bar{D}^0,J/\psi)\,;\\
\mathcal{A}(B_d\to\bar{D}^0\phi) &= V_{ud}V_{cb}^*\,EA_2(c,u,s;B_d,\bar{D}^0,\phi)\,, \qquad (47)
\end{aligned}$$

which would allow the extraction of A_2 and EA_2. To be able to extract A_1 one has to measure CKM suppressed decays such as the following:

$$\begin{aligned}
\mathcal{A}(B^+ \to D^+ K^0) &= V_{cs}V_{ub}^* A_1(s,d,c;B^+,K^0,D^+)\,; \\
\mathcal{A}(B^+ \to D_s^+ \phi) &= V_{cs}V_{ub}^* \Big(A_1(s,s,c;B^+,\phi,D_s^+) + EA_1(s,c,s;B^+,D_s^+,\phi)\Big)\,, \\
\mathcal{A}(B^+ \to D_s^+ J/\psi) &= V_{cs}V_{ub}^* \Big(A_1(s,c,c;B^+,D_s^+,J/\psi) + EA_1(s,c,c;B^+,D_s^+,J/\psi)\Big)\,. \qquad (48)
\end{aligned}$$

An example of decays proceeding through annihilations and penguin-annihilations is given by the following channels:

$$\begin{aligned}
\mathcal{A}(B_d \to D^0 \bar{D}^0) &= -V_{cd}V_{cb}^* A_2(c,u,c;B_d,\bar{D}^0,D^0) + V_{td}V_{tb}^* P_3(u,c;B_d,\bar{D}^0,D^0) \\
&\quad -V_{ud}V_{ub}^* \Big(A_2(u,c,u;B_d,D^0,\bar{D}^0) - P_3^{\rm GIM}(u,c;B_d,\bar{D}^0,D^0)\Big)\,; \\
\mathcal{A}(B_d \to D_s^+ D_s^-) &= V_{cd}V_{cb}^*\, A_2(c,s,c;B_d,D_s^-,D_s^+) - V_{ud}V_{ub}^*\, P_3^{\rm GIM}(c,s;B_d,D_s^+,D_s^-) \\
&\quad -V_{td}V_{tb}^*\, P_3(c,s;B_d,D_s^+,D_s^-)\,; \\
\mathcal{A}(B_d \to K^+ K^-) &= V_{ud}V_{ub}^* \Big(-A_2(u,s,u;B_d,K^-,K^+) + P_3^{\rm GIM}(u,s;B_d,K^+,K^-)\Big) \\
&\quad +V_{td}V_{tb}^*\, P_3(u,s;B_d,K^+,K^-)\,. \qquad (49)
\end{aligned}$$

The classification of B_d and B^+ decays is summarized in Tables 1 and 2 respectively.

8 Classification of Two-Body B_s Decays

The same formalism introduced in Sections 5 and 7 can be applied to B_s decays, and a classification of the various decay channels can be made according to the CKM structure and to the effective parameters entering the amplitude.

As in the previous Section, we present here the results obtained by neglecting terms that vanish in the limit of exact $SU(2)$ symmetry and discarding the effective parameters P_4 and $P_4^{\rm GIM}$, wherever it is justified to do so. The neglected terms, denoted in this Section by $\Delta\mathcal{A}$, can be found in Appendix A.

Class A decays

Class **A** decays are CKM-allowed penguin-free decay channels. We have:

$$\begin{aligned}
\mathcal{A}(B_s \to D_s^- \pi^+) &= V_{ud}V_{cb}^*\, E_1(d,u,c;B_s,\pi^+,D_s^-)\,; \\
\mathcal{A}(B_s \to \bar{D}^0 \bar{K}^0) &= V_{ud}V_{cb}^*\, E_2(c,u,d;B_s,\bar{D}^0,\bar{K}^0)\,. \qquad (50)
\end{aligned}$$

Other channels in class **A** are obtained by replacing pseudoscalar mesons with vector ones.

Class B decays

These are penguin-free CKM-suppressed decay channels. We have:

$$\begin{aligned}
\mathcal{A}(B_s \to D_s^- K^+) &= V_{us}V_{cb}^* \Big(E_1(s,u,c;B_s,K^+,D_s^-) + A_2(c,s,u;B_s,D_s^-,K^+)\Big)\,, \\
\mathcal{A}(B_s \to D_s^+ K^-) &= -V_{cs}V_{ub}^* \Big(E_1(s,c,u;B_s,D_s^+,K^-) + A_2(u,s,c;B_s,K^-,D_s^+)\Big)\,,
\end{aligned}$$

$$
\begin{aligned}
\mathcal{A}(B_s \to \bar{D}^0\phi) &= V_{us}V_{cb}^*\Big(E_2(c,u,s;B_s,\bar{D}^0,\phi) + EA_2(c,u,s;B_s,\bar{D}^0,\phi)\Big)\,,\\
\mathcal{A}(B_s \to D^0\phi) &= -V_{cs}V_{ub}^*\Big(E_2(u,c,s;B_s,D^0,\phi) + EA_2(u,c,s;B_s,D^0,\phi)\Big)\,.
\end{aligned}
\tag{51}
$$

Other class **B** decays are the following doubly-CKM-suppressed transitions:

$$
\begin{aligned}
\mathcal{A}(B_s \to D^+K^-) &= -V_{cd}V_{ub}^*E_1(d,c,u;B_s,D^+,K^-)\,;\\
\mathcal{A}(B_s \to D^0\bar{K}^0) &= -V_{cd}V_{ub}^*\,E_2(u,c,d;B_s,D^0,\bar{K}^0)\,;\\
\mathcal{A}(B_s \to \pi^0\phi) = &- \frac{V_{us}V_{ub}^*}{\sqrt{2}}\Big(E_2(u,u,s;B_s,\pi^0,\phi) + EA_2(u,u,s;B_s,\pi^0,\phi)\Big)\\
&- \frac{V_{ts}V_{tb}^*}{\sqrt{2}}\Big[P_2(s,d;B_s,\pi^0,\phi) - P_2(s,u;B_s,\pi^0,\phi)\Big] + \Delta\mathcal{A}(B_s \to \pi^0\phi)\,,
\end{aligned}
\tag{52}
$$

plus the corresponding ones with vector mesons. The term in square brackets in $\mathcal{A}(B_s \to \pi^0\phi)$ vanishes in the limit of exact isospin symmetry.

Class C decays

Class **C** decays are CKM-allowed channels in which penguin contributions are present (but not dominant). Here are some typical examples:

$$
\begin{aligned}
\mathcal{A}(B_s \to D_s^+D_s^-) &= V_{cs}V_{cb}^*\Big(E_1(s,c,c;B_s,D_s^+,D_s^-) + A_2(c,s,c;B_s,D_s^-,D_s^+)\Big) -\\
&\quad V_{ts}V_{tb}^*\Big(P_1(s,c;B_s,D_s^+,D_s^-) + P_3(c,s;B_s,D_s^+,D_s^-)\Big) -\\
&\quad V_{us}V_{ub}^*\Big(P_1^{\rm GIM}(s,c;B_s,D_s^+,D_s^-) + P_3^{\rm GIM}(c,s;B_s,D_s^+,D_s^-)\Big)\,;\\
\mathcal{A}(B_s \to J/\psi\phi) &= V_{cs}V_{cb}^*\Big(E_2(c,c,s;B_s,J/\psi,\phi) + EA_2(c,c,s;B_s,J/\psi,\phi)\Big)\\
&- V_{ts}V_{tb}^*\,P_2(s,c;B_s,J/\psi,\phi) - V_{us}V_{ub}^*\,P_2^{\rm GIM}(s,c;B_s,J/\psi,\phi)\\
&+ \Delta\mathcal{A}(B_s \to J/\psi\phi)\,.
\end{aligned}
\tag{53}
$$

Class D decays

Class **D** decays are CKM-suppressed decays in which penguin contributions are present:

$$
\begin{aligned}
\mathcal{A}(B_s \to \pi^0\bar{K}^0) = &- \frac{V_{ud}V_{ub}^*}{\sqrt{2}}\Big(E_2(u,u,d;B_s,\pi^0,\bar{K}^0) + P_1^{\rm GIM}(d,d;B_s,\pi^0,\bar{K}^0)\Big)\\
&- \frac{V_{td}V_{tb}^*}{\sqrt{2}}P_1(d,d;B_s,\pi^0,\bar{K}^0) + \Delta\mathcal{A}(B_s \to \pi^0\bar{K}^0)\,;\\
\mathcal{A}(B_s \to \pi^+K^-) = &- V_{ud}V_{ub}^*\Big(E_1(d,u,u;B_s,\pi^+,K^-) - P_1^{\rm GIM}(d,u;B_s,\pi^+,K^-)\Big)\\
&+ V_{td}V_{tb}^*\,P_1(d,u;B_s,\pi^+,K^-)\,;\\
\mathcal{A}(B_s \to D^+D_s^-) &= V_{cd}V_{cb}^*\,E_1(d,c,c;B_s,D^+,D_s^-) - V_{td}V_{tb}^*\,P_1(d,c;B_s,D^+,D_s^-) -\\
&\quad V_{ud}V_{ub}^*\,P_1^{\rm GIM}(d,c;B_s,D^+,D_s^-)\,;\\
\mathcal{A}(B_s \to \bar{K}^0J/\psi) &= V_{cd}V_{cb}^*\,E_2(c,c,d;B_s,J/\psi,\bar{K}^0) - V_{td}V_{tb}^*\,P_2(d,c;B_s,J/\psi,\bar{K}^0) -\\
&\quad V_{ud}V_{ub}^*\,P_2^{\rm GIM}(d,c;B_s,J/\psi,\bar{K}^0)\,.
\end{aligned}
\tag{54}
$$

Class E decays

This class contains channels in which penguin contributions are CKM-allowed, while non-penguin ones are either absent:

$$\begin{aligned}
\mathcal{A}(B_s \to K^0\bar{K}^0) = &- V_{us}V_{ub}^*\Big(P_1^{\rm GIM}(s,d;B_s,K^0,\bar{K}^0) + P_3^{\rm GIM}(d,s;B_s,K^0,\bar{K}^0)\Big)\\
&- V_{ts}V_{tb}^*\Big(P_1(s,d;B_s,K^0,\bar{K}^0) + P_3(d,s;B_s,K^0,\bar{K}^0)\Big)\,;\\
\sqrt{2}\mathcal{A}(B_s \to \phi\phi) = &- V_{us}V_{ub}^*\Big(2P_1^{\rm GIM}(s,s;B_s,\phi,\phi) + 2P_2^{\rm GIM}(s,s;B_s,\phi,\phi) + P_3^{\rm GIM}(s,s;B_s,\phi,\phi)\Big)\\
&- V_{ts}V_{tb}^*\Big(2P_1(s,s;B_s,\phi,\phi) + 2P_2(s,s;B_s,\phi,\phi) + P_3(s,s;B_s,\phi,\phi)\Big)\\
&+ \Delta\mathcal{A}(B_s \to \phi\phi)\,;
\end{aligned} \tag{55}$$

or doubly CKM-suppressed:

$$\begin{aligned}
\mathcal{A}(B_s \to \pi^+\pi^-) = &+ V_{us}V_{ub}^*\Big(P_3^{\rm GIM}(u,d;B_s,\pi^+,\pi^-) - A_2(u,d,u;B_s,\pi^-,\pi^+)\Big)\\
&+ V_{ts}V_{tb}^*\,P_3(u,d;B_s,\pi^+,\pi^-)\,;\\
\sqrt{2}\mathcal{A}(B_s \to \pi^0\pi^0) = &- V_{us}V_{ub}^*\Big(\frac{1}{2}P_3^{\rm GIM}(u,u;B_s,\pi^0,\pi^0) + \frac{1}{2}P_3^{\rm GIM}(d,d;B_s,\pi^0,\pi^0)\\
&\qquad -A_2(u,u,u;B_s,\pi^0,\pi^0)\Big)\\
&- V_{ts}V_{tb}^*\Big(\frac{1}{2}P_3(u,u;B_s,\pi^0,\pi^0) + \frac{1}{2}P_3(d,d;B_s,\pi^0,\pi^0)\Big) + \Delta\mathcal{A}(B_s \to \pi^0\pi^0)\,;\\
\mathcal{A}(B_s \to K^+K^-) = &- V_{us}V_{ub}^*\Big(E_1(s,u,u;B_s,K^+,K^-) + A_2(u,s,u;B_s,K^-,K^+) -\\
&\qquad P_1^{\rm GIM}(s,u;B_s,K^+,K^-) - P_3^{\rm GIM}(u,s;B_s,K^+,K^-)\Big)\\
&+ V_{ts}V_{tb}^*\Big(P_1(s,u;B_s,K^+,K^-) + P_3(u,s;B_s,K^+,K^-)\Big)\,.
\end{aligned} \tag{56}$$

Class F decays

The following channel is an example of a CKM-suppressed, pure penguin decay:

$$\begin{aligned}
\mathcal{A}(B_s \to \bar{K}^0\phi) = &- V_{td}V_{tb}^*\Big(P_1(d,s;B_s,\bar{K}^0,\phi) + P_2(d,s;B_s,\phi,\bar{K}^0)\Big)\\
&- V_{ud}V_{ub}^*\Big(P_1^{\rm GIM}(d,s;B_s,\bar{K}^0,\phi) + P_2^{\rm GIM}(d,s;B_s,\phi,\bar{K}^0)\Big)\,.
\end{aligned} \tag{57}$$

Class G decays

The following channels are CKM-allowed decays that proceed only through annihilation and penguin-annihilation:

$$\begin{aligned}
\mathcal{A}(B_s \to D^-D^+) &= V_{cs}V_{cb}^*\,A_2(c,d,c;B_s,D^-,D^+) - V_{us}V_{ub}^*\,P_3^{\rm GIM}(d,c;B_s,D^-,D^+)\\
&\quad -V_{ts}V_{tb}^*\,P_3(d,c;B_s,D^-,D^+)\,;\\
\mathcal{A}(B_s \to D^0\bar{D}^0) &= -V_{cs}V_{cb}^*A_2(c,u,c;B_s,\bar{D}^0,D^0) + V_{ts}V_{tb}^*P_3(u,c;B_s,\bar{D}^0,D^0)\\
&\quad +V_{us}V_{ub}^*\Big(P_3^{\rm GIM}(u,c;B_s,\bar{D}^0,D^0) - A_2(u,c,u;B_s,D^0,\bar{D}^0)\Big)\,.
\end{aligned} \tag{58}$$

$B_s \to \pi^0 J/\psi$ is an annihilation channel dominated by electroweak (isospin-breaking) effects:

$$\mathcal{A}(B_s \to \pi^0 J/\psi) = + \frac{V_{cs}V_{cb}^*}{\sqrt{2}}\Big[EA_2(c,c,d;B_s,J/\psi,\pi^0) - EA_2(c,c,u;B_s,J/\psi,\pi^0)\Big]$$

$$
\begin{aligned}
&- \quad \frac{V_{ts}V_{tb}^*}{\sqrt{2}}\Big[P_4(d,c;B_s,\pi^0,J/\psi) - P_4(u,c;B_s,\pi^0,J/\psi)\Big] \\
&- \quad \frac{V_{us}V_{ub}^*}{\sqrt{2}}EA_2(u,u,c;B_s,\pi^0,J/\psi) + \Delta\mathcal{A}(B_s\to\pi^0 J/\psi)\,, \qquad (59)
\end{aligned}
$$

where the quantities in square brackets vanish in the $SU(2)$ limit.

Here are some examples of CKM-suppressed pure annihilation decays:

$$
\begin{aligned}
\mathcal{A}(B_s\to\pi^-D^+) &= -V_{cs}V_{ub}^*\,A_2(u,d,c;B_s,\pi^-,D^+)\,; \\
\mathcal{A}(B_s\to\pi^+D^-) &= V_{us}V_{cb}^*\,A_2(c,d,u;B_s,D^-,\pi^+)\,; \\
\mathcal{A}(B_s\to J/\psi D^0) &= -V_{cs}V_{ub}^*\Big(A_2(u,c,c;B_s,D^0,J/\psi) + EA_2(u,c,c;B_s,D^0,J/\psi)\Big)\,; \\
\mathcal{A}(B_s\to J/\psi \bar D^0) &= V_{us}V_{cb}^*\Big(A_2(c,c,u;B_s,J/\psi,\bar D^0) + EA_2(c,u,c;B_s,\bar D^0,J/\psi)\Big)\,; \\
\mathcal{A}(B_s\to\pi^0D^0) &= \frac{V_{cs}V_{ub}^*}{\sqrt{2}}A_2(u,u,c;B_s,\pi^0,D^0) + \Delta\mathcal{A}(B_s\to\pi^0D^0)\,; \\
\mathcal{A}(B_s\to\pi^0\bar D^0) &= -\frac{V_{us}V_{cb}^*}{\sqrt{2}}A_2(c,u,u;B_s,\bar D^0,\pi^0) + \Delta\mathcal{A}(B_s\to\pi^0\bar D^0)\,. \qquad (60)
\end{aligned}
$$

The classification of B_s decays is summarized in Table 3.

9 Strategies for the experimental determination of the effective parameters

In this Section we would like to make general comments on the determination of the effective parameters from the data. A detailed numerical analysis will be presented in a subsequent work. The inspection of tables 1–3 allows to identify the most suitable decays for this determination. We have:

i) $|E_1|$ can be best determined from $B_d\to D^-K^+$, $D_s^+\pi^-$, $B^+\to D_s^+\pi^0$, $B_s\to D_s^-\pi^+$;

ii) $|E_2|$ can be extracted from $B_d\to D^0K^0$, $\bar D^0K^0$ and $B_s\to\bar D^0\bar K^0$;

iii) $|A_1|$ can be determined from $B^+\to D^+K^0$;

iv) $|A_2|$ can be taken from $B_s\to\pi^-D^+$, π^+D^-, π^0D^0, $\pi^0\bar D^0$;

v) $|EA_2|$ can be extracted from $B_d\to\bar D^0\phi$;

vi) $|P_1|$ can be determined from $B_d\to K^+\pi^-$, $K^0\pi^0$ and $B^+\to K^0\pi^+$, $K^+\pi^0$;

vii) $|P_3|$ can be extracted from $B_d\to\phi\phi$ and $B_s\to\pi^+\pi^-$.

In all these cases the parameter in question dominate a given decay or constitute the only contribution.

An independent determination of EA_1 and P_2 is harder:

viii) EA_1 could play some role in $B^+\to\pi^+J/\psi$, $\phi\pi^+$, $D_s^+\phi$, D_s^+J/ψ;

ix) P_2 could be non-negligible in $B^+\to J/\psi K^+$, $\phi\pi^+$ and in particular in $B_d\to J/\psi K^0$, $\phi\pi^0$, $B_s\to J/\psi\phi$ and $\phi\phi$. On the other hand, this contribution being $\mathcal{O}(1/N^2)$, it appears that this determination will only be possible by comparing various decays.

The determination of $P_i^{\rm GIM}$ is complicated by the fact that these contributions are often suppressed by $\mathcal{O}(\lambda^2)$ relatively to P_i contributions. However, in situations in which $P_i^{\rm GIM}$ are multiplied by CKM factors with large complex phases, as $V_{us}V_{ub}^*$, CP-asymmetries could be useful in this respect.

Finally we do not think that the parameters P_4 and $P_4^{\rm GIM}$ will be determined in the near future, as they are expected to be very small and one would need very precise data to investigate their effect.

When data will be available on most of the channels discussed in Sections 7 and 8, it will be possible to study the flavour dependence of the effective parameters and to learn more on final state interactions by extracting the phases of the effective parameters from the data.

10 Comparison with the Diagrammatic Approach

We will now compare our approach with the diagrammatic approach of refs. [17, 18], in particular with the formulation given in [18].

The main difference between these two approaches is the following one. Whereas the diagrammatic approach of [18] is formulated in terms of diagrams with full W, Z and top quark exchanges, the approach presented here is formulated directly in terms of local operators, the basic objects of the effective theory. The main advantages of formulating non-leptonic decays in terms of operators are as follows:

i) The effective parameters introduced in Section 4 are directly expressed in terms of matrix elements of local operators. Therefore they can be in principle calculated in QCD by means of suitable non-perturbative methods. Consequently the comparison of phenomenologically extracted effective parameters from the data with the values calculated in QCD may offer some useful tests and teach us something about strong interactions. Such tests are clearly not possible in the approach of [18] as no prescription is given on how the phenomenological parameters in this approach could be calculated in QCD.

ii) The inclusion of QCD perturbative corrections can be consistently performed by using the NLO Wilson coefficients in $\mathcal{H}_{\rm eff}$.

iii) The issues of renormalization scheme dependences, non-factorizable contributions, flavour dependences and in particular the important issue of final state interactions can be addressed transparently in the operator approach, whereas the diagrammatic approach can be in this context sometimes even misleading.

Several of these advantages cannot be fully appreciated yet in view of the limitations of present non-perturbative methods, but this may improve in the future.

In spite of these basic differences between our approach and the one in refs. [17, 18], it is possible to establish some connections between them and to show explicitly where they differ from each other.

In the approach of ref. [18] the basic parameters for strangeness-preserving decays are the "Tree" (colour favoured) amplitude T, the "colour suppressed" amplitude C, the "penguin" amplitude P, the "exchange" amplitude E, the "annihilation" amplitude A and the "penguin annihilation" amplitude PA. For strangeness-changing decays one has T', C', P', E', A', PA'. If Z-penguins are taken into account one introduces in addition the "colour-allowed" Z-penguin $P_{\rm EW}$ and the "colour-suppressed" Z-penguin $P_{\rm EW}^C$. Similarly $P'_{\rm EW}$ and $P'^C_{\rm EW}$ are introduced for strangeness-changing decays. All these amplitudes include the relevant CKM factors, whereas in our approach the CKM factors are not included

in the effective parameters. While this distinction is important for phenomenological applications, we will omit the CKM parameters in the discussion below, as far as possible.

Let us investigate how the parameters of ref. [18] are related to the parameters introduced in Section 4. It is sufficient to consider "unprimed" amplitudes. The discussion of "primed" amplitudes is completely analogous.

As stated above, the amplitudes T, C, P, E, A, PA, $P_{\rm EW}$ and $P^C_{\rm EW}$ are defined in terms of diagrams in the full theory which contain explicit W, Z and top propagators, whereas our approach is formulated in terms of operators and diagrams in the effective theory. The connection between these two approaches can be established by noting that in all diagrams of ref. [18] a W propagator is present, whereas in our approach the operator Q_1 contributes to all the effective parameters. Since a W-exchange between two quark lines is represented in the effective theory by Q_1 this is not surprising.

Now, the situation is of course more complicated as QCD corrections to a W-exchange generate other operators for which no diagrams exist in the diagrammatic approach of ref. [18]. In the limit $\alpha_s = 0$, $\alpha = 0$ we have, however, $C_1 = 1$ and $C_i = 0$ $(i \neq 1)$. Consequently in this particular limit the effective parameters in our approach are entirely given in terms of matrix elements of Q_1 and the correspondence between our approach and the one of ref. [18] is easier to establish. One can then think that when QCD and QED corrections are included, the contributions of the operators Q_i $(i \neq 1)$ are added properly to those of Q_1 so that the effective parameters are scale and renormalization scheme independent.

Proceeding in this manner it is easy to establish first the following correspondence

$$T \leftrightarrow E_1,\ C \leftrightarrow E_2,\ A \leftrightarrow A_1,\ E \leftrightarrow A_2. \tag{61}$$

The Zweig-suppressed contributions represented in our approach by EA_1 and EA_2 have not been taken into account in [18], although it is straightforward to draw the corresponding diagrams. In the case of charmless B-decays to two pseudoscalars, considered in [18], it is very plausible that these contributions can be neglected as seen in tables 1–3. On the other hand EA_1 could be important for $B^+ \to \phi\pi^+$ and in particular in decays with charm in the final state such as $B^+ \to \pi^+ J/\psi$, $D_s^+\phi$ and $D_s^+ J/\psi$. EA_2 is fully responsible for $B_d \to \bar{D}^0\phi$ and could be significant in $B_d \to \pi^0 J/\psi$, $B_s \to \bar{D}^0\phi$, $D^0\phi$, $J/\psi\phi$, $J/\psi D^0$.

The case of P, PA, $P_{\rm EW}$ and $P^C_{\rm EW}$ is more involved. If one sets $\alpha = 0$ we have roughly speaking

$$P \leftrightarrow P_1, \qquad PA \leftrightarrow P_3, \tag{62}$$

but this correspondence is a bit oversimplified and requires some explanation. It is sufficient to discuss only the first relation.

Let us write P as

$$P = V_{ud}V_{ub}^*\,(P_u - P_c) + V_{td}V_{tb}^*\,(P_t - P_c)\,, \tag{63}$$

where we have used the unitarity of the CKM matrix. In the language of ref. [18] P_u, P_c and P_t denote QCD penguin diagrams with internal u, c and t exchanges. As discussed already in [24, 27], in the operator approach P_t is represented by the contributions of the QCD penguin operators Q_{3-6} whereas P_u and P_c by the matrix elements $\langle Q_1\rangle^u_{CP}$ ($\langle Q_2\rangle^u_{DP}$) and $\langle Q_1\rangle^c_{CP}$ ($\langle Q_2\rangle^c_{DP}$) respectively. Thus we can establish the relation

$$P_c - P_t \leftrightarrow P_1, \qquad P_c - P_u \leftrightarrow P_1^{\rm GIM}. \tag{64}$$

At this point, following [24], it should be emphasized that whereas P_1 and $P_1^{\rm GIM}$ are μ and renormalization scheme independent, this is not the case for P_u, P_c and P_t. Consequently while $P_1^{\rm GIM}$ could possibly be neglected with respect to P_1, the neglect of P_c with respect to P_t or of P_u with respect to P_c would automatically introduce unphysical scheme dependences.

In this context we would like to recall that the impact of P_c and P_u on the extraction of CKM-phases has been investigated for the first time in [33]. In the operator language, the importance of the charm contribution to P_1 ("charming penguins") in connection with the CLEO data on $B \to K\pi$ has been stressed in [26] and analyzed in detail in [34]. Finally the role of P_u in connection with final state interactions in B decays has been pointed out in [24] and analyzed subsequently in [20]-[23], [25].

Let us now discuss the issue of electroweak penguin contributions which in the approach of ref. [18] are represented by $P_{\rm EW}$ and $P_{\rm EW}^C$. It is sufficient to discuss $P_{\rm EW}$ only. As in the case of P one can write

$$P_{\rm EW} = V_{ud}V_{ub}^* \left(P_{\rm EW}^u - P_{\rm EW}^c\right) + V_{td}V_{tb}^* \left(P_{\rm EW}^t - P_{\rm EW}^c\right), \tag{65}$$

where in the language of ref. [24, 27, 35] $P_{\rm EW}^u$, $P_{\rm EW}^c$ and $P_{\rm EW}^t$ denote Z-penguin diagrams with internal u, c and t exchanges. Strictly speaking $P_{\rm EW}^i$ have to include also the box contributions to make them gauge independent.

In our approach the electroweak penguin contributions are represented by the electroweak penguin operators Q_{7-10}, which are included in P_1 and in the other penguin parameters P_i. The point is that the contributions of Q_{7-10} are by themselves scale and renormalization scheme dependent and have to be considered simultaneously with other operators to obtain physical scheme independent results. Consequently when electroweak penguin contributions and generally $\mathcal{O}(\alpha)$ effects are included the correspondences (64) generalize to

$$P_c - P_t + P_{\rm EW}^c - P_{\rm EW}^t \leftrightarrow P_1, \qquad P_c - P_u + P_{\rm EW}^c - P_{\rm EW}^u \leftrightarrow P_1^{\rm GIM}\,, \tag{66}$$

with

$$P_c + P_{\rm EW}^c \leftrightarrow C_1\langle Q_1\rangle_{CP}^c + C_2\langle Q_2\rangle_{DP}^c, \qquad P_u + P_{\rm EW}^u \leftrightarrow C_1\langle Q_1\rangle_{CP}^u + C_2\langle Q_2\rangle_{DP}^u\,. \tag{67}$$

Here $\langle Q_1\rangle_{CP}^c$ includes the insertion of Q_1 in the CP penguin topology both with gluon exchanges and with a single photon exchange. It can be considered as a sum of QCD charming penguins and QED charming penguins. Similar comments apply to $\langle Q_2\rangle_{DP}^c$, $\langle Q_1\rangle_{CP}^u$ and $\langle Q_2\rangle_{DP}^u$. The QED charming penguins as well as the QED u-penguins have been identified in [27] but neglected with respect to top penguins represented in our approach dominantly by the contributions of the operators Q_9 and Q_{10}. Note that $C_{1,2} = \mathcal{O}(1)$ whereas $\langle Q_1\rangle_{CP}^{c,u}$ and $\langle Q_2\rangle_{DP}^{c,u}$ with a single photon exchange are $\mathcal{O}(\alpha)$. On the other hand C_9 and C_{10} are $\mathcal{O}(\alpha)$ but $\langle Q_9\rangle_{CE}$ and $\langle Q_{10}\rangle_{DE}$ contributing to P_1 in (11) are $\mathcal{O}(1)$. Thus from the point of view of an expansion in α the QED c- and u-penguin insertions of Q_1 and Q_2 are of the same order as the Q_9 and the Q_{10} contributions. In fact, as we stated above, they have to be both included in order to obtain scheme independent results. On the other hand one could argue that the strong enhancement of $C_{9,10}$ through the large top quark mass and the suppression of $\langle Q_1\rangle_{CP}^{c,u}$ and $\langle Q_2\rangle_{DP}^{c,u}$ through $1/16\pi^2$ factors present in a perturbative evaluation of these matrix elements makes the neglect of QED c- and u-penguin insertions of Q_1 and Q_2 plausible. This is supported to some extent by the very weak scheme dependence of C_9 and C_{10}. Still one should keep in mind that perturbative arguments for the smallness of $\mathcal{O}(\alpha)$ corrections to $\langle Q_1\rangle_{CP}^{c,u}$ and $\langle Q_2\rangle_{DP}^{c,u}$ may not apply and the relevance of these contributions has been possibly underestimated in the literature so far.

The Zweig-suppressed penguin contributions represented in our approach by P_2 and P_4 have not been taken into account in [18]. As in the case of EA_1 and EA_2 their role in charmless B decays to two pseudoscalars is expected to be very small. As seen in tables 1-3, P_2 could play some role in a number of decays with charm in the final state, in $B_d \to \phi\pi^0$, $K^0\phi$ and analogous channels in B^+ and B_s decays. P_4 being doubly Zweig-suppressed is most probably negligible in all decays.

Finally we would like to comment on the parameters P, T, $P^C_{\rm EW}$, C etc. used in refs. [24, 27, 35]. These parameters should not be confused with the ones discussed above. They have been introduced in order to make the analysis of the extraction of the angle γ from $B \to K\pi$ decays more transparent. As an example we show how the parameters P, T and $P^C_{\rm EW}$ defined through

$$\mathcal{A}(B^+ \to \pi^+ K^0) = P\,, \qquad \mathcal{A}(B_d \to \pi^- K^+) = -(P + T + P^C_{\rm EW}) \tag{68}$$

are given in terms of the effective parameters introduced in Sections 4 and 5. One has

$$\begin{aligned}
P &= V_{us}V_{ub}^*\Big(A_1(s,d,u;B^+,K^0,\pi^+) - P_1^{\rm GIM}(s,d;B^+,K^0,\pi^+)\Big) - V_{ts}V_{tb}^*\,P_1(s,d;B^+,K^0,\pi^+)\,,\\
P^C_{\rm EW} &= -V_{cs}V_{cb}^*\Big[P_1(s,d;B^+,K^0,\pi^+) - P_1(s,u;B_d,K^+,\pi^-)\Big]\,,\\
T &= V_{us}V_{ub}^*\Big\{E_1(s,u,u;B_d,K^+,\pi^-) - A_1(s,d,u;B^+,K^0,\pi^+)\\
&\quad + \Big[P_1^{\rm GIM}(s,d;B^+,K^0,\pi^+) - P_1^{\rm GIM}(s,u;B_d,K^+,\pi^-)\Big]\\
&\quad - \Big[P_1(s,d;B^+,K^0,\pi^+) - P_1(s,u;B_d,K^+,\pi^-)\Big]\Big\}\,,
\end{aligned} \tag{69}$$

where λ and A are the Wolfenstein parameters.

Analogous expressions can be found for other $B \to K\pi$ decays.

11 Summary

In the present paper we have proposed a general framework for analyzing non-leptonic two-body B-decays which combines the operator language with the diagrammatic language. Following and generalizing the discussion of ref. [26] we have classified the contributions to the matrix elements of the relevant operators in terms of different topologies of Wick contractions. Subsequently we have introduced a set of effective parameters which are both renormalization scale and renormalization scheme independent. As such they are convenient for phenomenological applications.

On the other hand, being linear combinations of Wilson coefficients and particular Wick contractions of local operators, these effective parameters are in principle calculable in QCD. This feature distinguishes our approach from the diagrammatic approach of refs. [17, 18] in which no reference to local operators is made and no prescription for the calculation of the corresponding parameters is given.

The formulation given here allows to describe in general terms the flavour dependence of non-leptonic two-body decays including non-factorizable contributions and final state interactions. It is therefore particularly useful for a general model-independent study of CP violation in B decays.

In the present paper we did not use any symmetry arguments like $SU(2)$ or $SU(3)$ flavour symmetries. On the other hand we have used the $1/N$ expansion to indicate a possible hierarchy among the effective parameters. In particular we have included in our discussion a number of Zweig-suppressed

topologies, which have not been discussed in the literature. We have shown that these topologies have to be included in order to obtain a consistent description of non-leptonic decays with respect to scale and renormalization scheme dependences. While such topologies are suppressed in the large N limit, the role of Zweig-suppressed contributions in non-leptonic decays is an interesting and important issue, which requires further theoretical and phenomenological investigations.

As a preparation for phenomenological applications of our formalism we have presented a classification of two-body B decay channels according to the effective parameters entering in the decay amplitudes. This classification enabled us to identify subsets of channels that, when measured, would allow a direct determination of the effective parameters making no assumption about non-factorizable contributions and rescattering. The execution of this program is deferred to a subsequent work.

The approach presented here allows for a phenomenological description of non-leptonic decays, once a large number of channels have been measured. Such a description may teach us about the role of non-factorizable contributions and about the flavour structure of non-leptonic B decays. One should hope that in this manner some regularities will be found. However, without a dynamical input the formulation presented so far can be considered only as the most suitable language to describe non-leptonic decays in a manner consistent with QCD. In order to be predictive some additional input involving symmetry arguments and dynamical assumptions is needed. We will return to these issues in a subsequent publication.

Acknowledgments

We would like to thank Stefan Bosch for invaluable comments on the manuscript and for checking many equations. We also thank A. Khodjamirian for discussions.

A Remaining Contributions

We collect here the contributions that were neglected in the analyses of Sections 7 and 8. These include the terms proportional to P_4 and $P_4^{\rm GIM}$, and some of the terms vanishing in the limit of $SU(2)$. The $SU(2)$ breaking effects come on the one hand from the matrix elements of electroweak penguin operators, and on the other hand from $O(\alpha)$ effects in the matrix elements of operators Q_{1-6}. We stress that, for consistency, if one takes into account the effects of electroweak penguin operators, one should also include $O(\alpha)$ effects in the matrix elements of operators Q_{1-6}. Therefore, in this case operators Q_{3-6} can also contribute to $\Delta I = 1$ (or 3/2) transitions, due to $O(\alpha)$ effects in the matrix elements. These contributions will be, for example, of the form $P_1(d,u;B^+,\pi^+,\pi^0) - P_1(d,d;B^+,\pi^0,\pi^+)$, vanishing in the $SU(2)$ symmetric limit, and will be proportional to α. Thus, while the individual P_i penguin parameters are of order α_s, differences of penguin parameters vanishing in the $SU(2)$ symmetric limit are at least of order α.

Class A decays

We have (here and in the following we give results in units of $G_F/\sqrt{2}$):

$$\Delta\mathcal{A}(B_d \to \bar{D}^0\pi^0) \;=\; \frac{V_{ud}V_{cb}^*}{\sqrt{2}}\Big[EA_2(c,u,d;B_d,\bar{D}^0,\pi^0) - EA_2(c,u,u;B_d,\bar{D}^0,\pi^0)\Big]\,. \qquad (70)$$

Class B decays

We have:

$$\begin{aligned}
\Delta\mathcal{A}(B^+ \to D_s^+\pi^0) &= -\frac{V_{cs}V_{ub}^*}{\sqrt{2}}\Big[EA_1(s,c,u;B^+,D_s^+,\pi^0) - EA_1(s,c,d;B^+,D_s^+,\pi^0)\Big]\,, \\
\Delta\mathcal{A}(B_s \to \pi^0\phi) = &- \frac{V_{us}V_{ub}^*}{\sqrt{2}}\Bigg(\Big[P_2^{\rm GIM}(s,d;B_s,\pi^0,\phi) - P_2^{\rm GIM}(s,u;B_s,\pi^0,\phi)\Big] \\
&+ \Big[P_4^{\rm GIM}(d,s;B_s,\pi^0,\phi) - P_4^{\rm GIM}(u,s;B_s,\pi^0,\phi)\Big]\Bigg) \\
&- \frac{V_{ts}V_{tb}^*}{\sqrt{2}}\Big[P_4(d,s;B_s,\pi^0,\phi) - P_4(u,s;B_s,\pi^0,\phi)\Big]\,. \qquad (71)
\end{aligned}$$

Class C decays

We have:

$$\Delta\mathcal{A}(B_s \to J/\psi\phi) = -V_{ts}V_{tb}^*P_4(c,s;B_s,J/\psi,\phi) - V_{us}V_{ub}^*P_4^{\rm GIM}(c,s;B_s,J/\psi,\phi)\,. \qquad (72)$$

Class D decays

We have:

$$\begin{aligned}
\Delta\mathcal{A}(B_d \to \pi^0\pi^0) = &- V_{ud}V_{ub}^*\Bigg(\Big[EA_2(u,u,d;B_d,\pi^0,\pi^0) - EA_2(u,u,u;B_d,\pi^0,\pi^0)\Big] \\
&+ \Big[\frac{1}{2}P_4^{\rm GIM}(u,u;B_d,\pi^0,\pi^0) - P_4^{\rm GIM}(u,d;B_d,\pi^0,\pi^0) + \frac{1}{2}P_4^{\rm GIM}(d,d;B_d,\pi^0,\pi^0)\Big] \\
&- \Big[P_2^{\rm GIM}(d,u;B_d,\pi^0,\pi^0) - P_2^{\rm GIM}(d,d;B_d,\pi^0,\pi^0)\Big]\Bigg) \\
&- V_{td}V_{tb}^*\Bigg(\Big[\frac{1}{2}P_4(u,u;B_d,\pi^0,\pi^0) - P_4(u,d;B_d,\pi^0,\pi^0) + \frac{1}{2}P_4(d,d;B_d,\pi^0,\pi^0)\Big] \\
&- \Big[P_2(d,u;B_d,\pi^0,\pi^0) - P_2(d,d;B_d,\pi^0,\pi^0)\Big]\Bigg)\,; \\
\Delta\mathcal{A}(B_d \to \pi^0 J/\psi) = &+ \frac{V_{cd}V_{cb}^*}{\sqrt{2}}\Big[EA_2(c,c,d;B_d,J/\psi,\pi^0) - EA_2(c,c,u;B_d,J/\psi,\pi^0)\Big] \\
&- \frac{V_{ud}V_{ub}^*}{\sqrt{2}}\Big[P_4^{\rm GIM}(d,c;B_d,\pi^0,J/\psi) - P_4^{\rm GIM}(u,c;B_d,\pi^0,J/\psi)\Big] \\
&+ \frac{V_{td}V_{tb}^*}{\sqrt{2}}\Big[P_4(u,c;B_d,\pi^0,J/\psi) - P_4(d,c;B_d,\pi^0,J/\psi)\Big]\,; \\
\Delta\mathcal{A}(B^+ \to \pi^+\pi^0) = &+ \frac{V_{ud}V_{ub}^*}{\sqrt{2}}\Bigg(\Big[A_1(d,d,u;B^+,\pi^0,\pi^+) - A_1(d,u,u;B^+,\pi^+,\pi^0)\Big] + \\
&\qquad \Big[EA_1(d,u,d;B^+,\pi^+,\pi^0) - EA_1(d,u,u;B^+,\pi^+,\pi^0)\Big] - \\
&\qquad \Big[P_1^{\rm GIM}(d,d;B^+,\pi^0,\pi^+) - P_1^{\rm GIM}(d,u;B^+,\pi^+,\pi^0)\Big] + \\
&\qquad \Big[P_2^{\rm GIM}(d,u;B^+,\pi^0,\pi^+) - P_2^{\rm GIM}(d,d;B^+,\pi^0,\pi^+)\Big]\Bigg)\,;
\end{aligned}$$

$$\begin{aligned}
\Delta\mathcal{A}(B_s\to\pi^0\bar{K}^0) = &- \frac{V_{ud}V_{ub}^*}{\sqrt{2}}\Big[P_2^{\rm GIM}(d,d;B_s,\pi^0,\bar{K}^0) - P_2^{\rm GIM}(d,u;B_s,\pi^0,\bar{K}^0)\Big] \\
&- \frac{V_{td}V_{tb}^*}{\sqrt{2}}\Big[P_2(d,d;B_s,\pi^0,\bar{K}^0) - P_2(d,u;B_s,\pi^0,\bar{K}^0)\Big]\,. \qquad (73)
\end{aligned}$$

Class E decays

We have:

$$\begin{aligned}
\Delta\mathcal{A}(B_d\to K^0\pi^0) = &- \frac{V_{us}V_{ub}^*}{\sqrt{2}}\Big[P_2^{\rm GIM}(s,d;B_d,\pi^0,K^0) - P_2^{\rm GIM}(s,u;B_d,\pi^0,K^0)\Big] \\
&- \frac{V_{ts}V_{tb}^*}{\sqrt{2}}\Big[P_2(s,d;B_d,\pi^0,K^0) - P_2(s,u;B_d,\pi^0,K^0)\Big]\,; \\
\Delta\mathcal{A}(B^+\to K^+\pi^0) = &- \frac{V_{us}V_{ub}^*}{\sqrt{2}}\Bigg(\Big[EA_1(s,u,u;B^+,K^+,\pi^0) - EA_1(s,u,d;B^+,K^+,\pi^0)\Big] + \\
&\qquad\Big[P_2^{\rm GIM}(s,d;B^+,\pi^0,K^+) - P_2^{\rm GIM}(s,u;B^+,\pi^0,K^+)\Big]\Bigg) \\
&- \frac{V_{ts}V_{tb}^*}{\sqrt{2}}\Big[P_2(s,d;B^+,\pi^0,K^+) - P_2(s,u;B^+,\pi^0,K^+)\Big]\Bigg)\,; \\
\Delta\mathcal{A}(B_s\to\phi\phi) = &- V_{us}V_{ub}^*\,P_4^{\rm GIM}(s,s;B_s,\phi,\phi) - V_{ts}V_{tb}^*\,P_4(s,s;B_s,\phi,\phi)\,; \\
\Delta\mathcal{A}(B_s\to\pi^0\pi^0) = &- V_{us}V_{ub}^*\Bigg(\Big[\frac{1}{2}P_4^{\rm GIM}(u,u;B_s,\pi^0,\pi^0) + \frac{1}{2}P_4^{\rm GIM}(d,d;B_s,\pi^0,\pi^0) - \\
&\qquad P_4^{\rm GIM}(u,d;B_s,\pi^0,\pi^0)\Big] + \Big[EA_2(u,u,d;B_s,\pi^0,\pi^0) - EA_2(u,u,u;B_s,\pi^0,\pi^0)\Big]\Bigg) \\
&- V_{ts}V_{tb}^*\Big[\frac{1}{2}P_4(u,u;B_s,\pi^0,\pi^0) + \frac{1}{2}P_4(d,d;B_s,\pi^0,\pi^0) - P_4(u,d;B_s,\pi^0,\pi^0)\Big]\,. \qquad (74)
\end{aligned}$$

Class F decays

We have:

$$\begin{aligned}
\Delta\mathcal{A}(B_d\to\phi\pi^0) = &+ \frac{V_{td}V_{tb}^*}{\sqrt{2}}\Big[P_4(u,s;B_d,\pi^0,\phi) - P_4(d,s;B_d,\pi^0,\phi)\Big] \\
&+ \frac{V_{ud}V_{ub}^*}{\sqrt{2}}\Big[P_4^{\rm GIM}(u,s;B_d,\pi^0,\phi) - P_4^{\rm GIM}(d,s;B_d,\pi^0,\phi)\Big]\,; \\
\Delta\mathcal{A}(B_d\to\phi\phi) = &- V_{td}V_{tb}^*\,P_4(s,s;B_d,\phi,\phi) - V_{ud}V_{ub}^*\,P_4^{\rm GIM}(s,s;B_d,\phi,\phi)\,. \qquad (75)
\end{aligned}$$

Class G decays

We have:

$$\begin{aligned}
\Delta\mathcal{A}(B_s\to\pi^0 J/\psi) = &- \frac{V_{us}V_{ub}^*}{\sqrt{2}}\Big[P_4^{\rm GIM}(d,c;B_s,\pi^0,J/\psi) - P_4^{\rm GIM}(u,c;B_s,\pi^0,J/\psi)\Big]\,; \\
\Delta\mathcal{A}(B_s\to\pi^0 D^0) = &\ \frac{V_{cs}V_{ub}^*}{\sqrt{2}}\Big[EA_2(u,c,u;B_s,D^0,\pi^0) - EA_2(u,c,d;B_s,D^0,\pi^0)\Big]\,; \\
\Delta\mathcal{A}(B_s\to\pi^0 \bar{D}^0) = &- \frac{V_{us}V_{cb}^*}{\sqrt{2}}\Big[EA_2(c,u,u;B_s,\bar{D}^0,\pi^0) - EA_2(c,u,d;B_s,\bar{D}^0,\pi^0)\Big]\,. \qquad (76)
\end{aligned}$$

References

[1] G. Altarelli, G. Curci, G. Martinelli and S. Petrarca, *Nucl. Phys.* **B 187** (1981) 461;
A.J. Buras and P.H. Weisz, *Nucl. Phys.* **B 333** (1990) 66.

[2] A.J. Buras, M. Jamin, M.E. Lautenbacher and P.H. Weisz, *Nucl. Phys.* **B 370** (1992) 69; *Nucl. Phys.* **B 400** (1993) 37;
A.J. Buras, M. Jamin and M.E. Lautenbacher, *Nucl. Phys.* **B 400** (1993) 75; *Nucl. Phys.* **B 408** (1993) 209.

[3] M. Ciuchini, E. Franco, G. Martinelli and L. Reina, *Phys. Lett.* **B 301** (1993) 263; *Nucl. Phys.* **B 415** (1994) 403.

[4] L. Maiani and M. Testa, *Phys. Lett.* **B 245** (1990) 585.

[5] M. Ciuchini, E. Franco, G. Martinelli and L. Silvestrini, *Phys. Lett.* **B 380** (1996) 353;
L. Silvestrini, *Nucl. Phys. Proc. Suppl.* **54A** (1997) 276.

[6] J. Schwinger, *Phys. Rev. Lett.* **12** (1964) 630;
R.P. Feynman, in *Symmetries in Particle Physics*, ed. A. Zichichi, Acad. Press 1965, p.167;
O. Haan and B. Stech, *Nucl. Phys.* **B 22** (1970) 448;
D. Fakirov and B. Stech, *Nucl. Phys.* **B 133** (1978) 315;
L.L. Chau, *Phys. Rep.* **95** (1983) 1.

[7] M. Wirbel, B. Stech and M. Bauer, *Zeit. für Physik* **C 29** (1985) 637;
M. Bauer, B. Stech and M. Wirbel, *Zeit. für Physik* **C 34** (1987) 103.

[8] M. Neubert, V. Rieckert, B. Stech and Q.P. Xu, in "Heavy Flavours", eds. A.J. Buras and M. Lindner (World Scientific, Singapore, 1992), p. 286.

[9] D. Du and Z. Xing, *Phys. Lett.* **B 312** (1993) 199;
A. Deandrea et al., *Phys. Lett.* **B 318** (1993) 549; *Phys. Lett.* **B 320** (1994) 170;
F. Buccella, F. Lombardi, G. Miele and P. Santorelli, *Zeit. für Physik* **C 59** (1993) 437;
N.G. Deshpande, B. Dutta and S. Oh, *Phys. Rev.* **D 57** (1998) 5723; `hep-ph/9712445`.

[10] M. Neubert and B. Stech, Preprint CERN-TH/97-99, `hep-ph/9705292`, to appear in Heavy Flavours II, edited by A.J. Buras and M. Lindner (World Scientific, Singapore);
B. Stech, in Honolulu 1997, B physics and CP violation, p. 140;
M. Neubert, *Nucl. Phys. Proc. Suppl.* **64** (1998) 474; `hep-ph/9801269`.

[11] A. Ali and C. Greub, *Phys. Rev.* **D 57** (1998) 2996;
A. Ali, J. Chay, C. Greub and P. Ko, *Phys. Lett.* **B 424** (1998) 161.

[12] A. Ali, G. Kramer and C.-D. Lü, *Phys. Rev.* **D 58** (1998) 094009.

[13] H.-Y. Cheng, *Phys. Lett.* **B 335** (1994) 428; *Phys. Lett.* **B 395** (1997) 345;
H.-Y. Cheng and B. Tseng, `hep-ph/9708211`; *Phys. Rev.* **D 58** (1998) 094005;
Y.-H. Chen, H.-Y. Cheng and B. Tseng, `hep-ph/9809364`;
H.-Y. Cheng and K.-C. Yang, `hep-ph/9811249`.

[14] J.M. Soares, *Phys. Rev.* **D 51** (1995) 3518.

[15] A.J. Buras and L. Silvestrini, Preprint TUM-HEP-315-98, `hep-ph/9806278`.

[16] M. Ciuchini, R. Contino, E. Franco and G. Martinelli, Rome preprint ROME1-1222/98, `hep-ph/9810271`.

[17] D. Zeppenfeld, *Zeit. für Physik* **C 8** (1981) 77;
A. Khodjamirian, *Sov. J. Nucl. Phys.* **30** (1997) 425;
L.L. Chau, *Phys. Rev.* **D 43** (1991) 2176.

[18] M. Gronau, J.L. Rosner and D. London, *Phys. Rev. Lett.* **73** (1994) 21;
O.F. Hernandez, M. Gronau, J.L. Rosner and D. London, *Phys. Lett.* **B 333** (1994) 500; *Phys. Rev.* **D 50** (1994) 4529.

[19] L. Wolfenstein, *Phys. Rev.* **D 52** (1995) 537;
J. Donoghue, E. Golowich, A. Petrov and J. Soares, *Phys. Rev. Lett.* **77** (1996) 2178;
B. Blok and I. Halperin, *Phys. Lett.* **B 385** (1996) 324;
B. Blok, M. Gronau and J.L. Rosner, *Phys. Rev. Lett.* **78** (1997) 3999;
P. Zenczykowski, *Acta Phys. Polon.* **B 28** (1997) 1605.

[20] J.-M. Gérard and J. Weyers, preprint UCL-IPT-97-18 (1997), `hep-ph/9711469`.

[21] A.F. Falk, A.L. Kagan, Y. Nir and A.A. Petrov, *Phys. Rev.* **D 57** (1998) 4290.

[22] D. Atwood and A. Soni, *Phys. Rev.* **D 58** (1998) 036005.

[23] M. Gronau and J.L. Rosner, *Phys. Rev.* **D 58** (1998) 113005.

[24] A.J. Buras, R. Fleischer and T. Mannel, *Nucl. Phys.* **B 533** (1998) 3.

[25] M. Neubert, *Phys. Lett.* **B 424** (1998) 152.

[26] M. Ciuchini, E. Franco, G. Martinelli and L. Silvestrini, *Nucl. Phys.* **B 501** (1997) 271.

[27] R. Fleischer, *Eur. Phys. J.* **C** (1998) DOI 10.1007/s100529800919 [`hep-ph/9802433`].

[28] B. Grinstein and R.F. Lebed, *Phys. Rev.* **D 53** (1996) 6344.

[29] B. Blok and M.A. Shifman, *Sov. J. Nucl. Phys.* **45** (1987) 135, 301, 522;
A. Khodjamirian and R. Rückl, in "Heavy Flavours", eds. A.J. Buras and M. Lindner (World Scientific, Singapore, 1992), p. 345;
B. Blok and M. Shifman, *Nucl. Phys.* **B 389** (1993) 534;
I. Halperin, *Phys. Lett.* **B 349** (1995) 548;
A. Khodjamirian and R. Rückl, `hep-ph/9807495`;
R. Rückl, `hep-ph/9810338`.

[30] G. Buchalla, A.J. Buras and M.E. Lautenbacher, *Rev. Mod. Phys.* **68** (1996) 1125.

[31] M. Gronau, *Phys. Lett.* **B 300** (1993) 163;
J.P. Silva and L. Wolfenstein, *Phys. Rev.* **D 49** (1994) 1151;
R. Aleksan, F. Buccella, A. Le Yaouanc, L. Oliver, O. Pene and J.C. Raynal, *Phys. Lett.* **B 356** (1995) 95;
F. DeJongh and P. Sphicas, *Phys. Rev.* **D 53** (1996) 1930;
P.S. Marrocchesi and N. Paver, *Int. J. Mod. Phys.* **A 13** (1998) 251;
J. Charles, preprint LPTHE-ORSAY-98-35, `hep-ph/9806468`.

[32] CLEO Collaboration (R. Godang et al.), *Phys. Rev. Lett.* **80** (1998) 3456.

[33] A.J. Buras and R. Fleischer, *Phys. Lett.* **B 341** (1995) 379.

[34] M. Ciuchini, R. Contino, E. Franco, G. Martinelli and L. Silvestrini, *Nucl. Phys.* **B 512** (1998) 3.

[35] A.J. Buras and R. Fleischer, CERN preprint CERN-TH/98-319, `hep-ph/9810260`.